

Light Out-Coupling Management in Perovskite LEDs—What Can We Learn from the Past?

Qianpeng Zhang, Daquan Zhang, Yu Fu, Swapnadeep Poddar, Lei Shu, Xiaoliang Mo, and Zhiyong Fan*

The research on perovskite light-emitting diodes (PeLEDs) has experienced an exponential growth in the past six years. The highest external quantum efficiencies (EQEs) have surpassed 20%, 20%, and 10% for red, green, and blue colored LEDs, respectively. Considering the internal quantum efficiency is already approaching unity owing to the high material quality, the limiting factor for further improving the EQE is mainly the poor light out-coupling efficiencies. Here, by reviewing the progress on the light out-coupling studies for PeLEDs, organic LEDs (OLEDs), conventional semiconductor LEDs, and other special LEDs, the rational design guidelines are summarized for enhancing PeLED out-coupling. Briefly, these design guidelines include: 1) introducing nanostructures into the active layer or tuning the thickness of it to couple out the waveguide modes, 2) adding nanostructures between the active layer and transparent electrodes to couple the waveguide modes to substrate modes, 3) adding nanostructures such as nanowires to the glass substrate to couple the substrate mode to air. Essentially, these guidelines indicate that implementing nanophotonic engineering on PeLEDs is a highly promising direction to explore, so as to substantially enhance the device performance.

perovskite materials have emerged as a highly promising class of materials for LEDs and have experienced rapid development owing to their superior optoelectronic properties.^[1] Particularly, for green, red and near-infrared (NIR) perovskite LEDs (PeLEDs), the external quantum efficiencies (EQEs) have all surpassed the 20% milestones.^[2] For blue PeLEDs, the EQE has exceeded 10%.^[3]

Among those state-of-art reports, Huang and co-workers used self-formed sub-micrometer structure and achieved 20.7% EQE for NIR PeLED;^[2a] Wei and co-workers utilized quasi-core/shell structure for 20.3% EQE green PeLED;^[2c] Chiba et al. reported the anion-exchange quantum dots (QDs) red PeLED with 21.3% EQE;^[2b] Jin and co-workers reported the quantum-confined bromide blue (at 483 nm) PeLED with 9.5% EQE;^[3a] Huang and co-workers achieved 11% EQE for sky-blue PeLED by incorporating yttrium into the perovskite grains.^[3c]

1. Introduction

Displays and lighting constitute two primary energy consuming sources in our daily life nowadays; therefore, it is of the utmost importance to keep developing new materials and technologies for energy efficient light-emitting diodes (LEDs) which are the fundamental building blocks for displays and lighting since the beginning of this century. In the past six years,

Moreover, Sargent and co-workers have thoroughly reviewed the development of PeLEDs from the material point-of-view,^[1c] and discussed the material engineering, interface engineering, and the stability issue. Besides, Friend and co-workers have discussed the physics of light emission in PeLEDs and talked about the photon generation and management particularly.^[1b] Basically, both high radiative efficiencies and efficient out-coupling of photons are required to maximize the EQE which is the key figure-of-merit for LEDs. Very intriguingly, the nonradiative decay pathways are related to the ion-migration, therefore solving one problem can simultaneously solve the other.^[4] Actually, inhibiting or even eliminating the ion-migration is another key to achieve stable PeLEDs,^[5] but it is beyond the scope of our discussions here. Furthermore, Stranks gave the following formula for the photoluminescent quantum yield (PLQY) of perovskites^[4]


$$\eta = \left[\frac{\eta_{\text{esc}}}{\eta_{\text{meas}}} + (1 - \eta_{\text{esc}}) \right]^{-1} \quad (1)$$

where the η is the internal PLQY, η_{meas} is the measured PLQY or the external PLQY, and η_{esc} is the photon escaping probability that can be interpreted as the out-coupling efficiency (OCE) in this review. (In this review, we will use OCE to

Dr. Q. Zhang, Dr. D. Zhang, Y. Fu, S. Poddar, L. Shu, Prof. Z. Fan
 Department of Electronic and Computer Engineering
 The Hong Kong University of Science and Technology
 Clear Water Bay, Hong Kong SAR, China
 E-mail: eezfan@ust.hk

Dr. D. Zhang, Y. Fu, Prof. Z. Fan
 HKUST-Shenzhen Research Institute
 No.9 Yuexing 1st RD, South Area, Hi-Tech Park, Nanshan
 Shenzhen 518057, China

Prof. X. Mo
 Department of Materials Science
 Fudan University
 Shanghai 200433, China

 The ORCID identification number(s) for the author(s) of this article can be found under <https://doi.org/10.1002/adfm.202002570>.

DOI: 10.1002/adfm.202002570

represent both photon escaping probability and light extraction efficiency (LEE) for the consistency.) Surprisingly, the OCE is only 12.7% for thin film MAPbI₃ on the glass.^[6] Regarding the photoluminescence (PL) of perovskite thin film, Herz and co-workers discussed the homogeneous PL spectrum broadening which can be attributed to the photon coupling.^[7]

Moreover, Stranks et al. proposed a few conditions to achieve high-efficiency PeLED.^[1b] First, the charge injection should be balanced. Second, the leakage current should be reduced. Third, the PLQY needs to be high. Last, the out-coupling of emitted light should be efficient. Moreover, the following formula for EQE was provided^[1b]

$$EQE = f_{\text{balance}} \times f_{e-h} \times \eta_{\text{radiative}} \times f_{\text{out-coupling}} \quad (2)$$

where the f_{balance} is the probability of balanced charge injection. The f_{e-h} is the probability of forming correlated electron-hole pair or exciton from each pair of injected carriers. The $\eta_{\text{radiative}}$ is the probability of radiative recombination for each electron-hole pair. Very importantly, the $f_{\text{out-coupling}}$ is the optical OCE. This formula gives us the basic guideline for PeLEDs performance improvement. The target of this review is to discuss how to improve the $f_{\text{out-coupling}}$ for PeLEDs.

In order to increase the OCE, nanophotonic engineering is one of the most effective strategies. Because the internal quantum efficiency (IQE) of perovskites, which can be estimated by PLQYs, is already approaching unity,^[8] the light OCE has become the most critical limiting factor for further device performance enhancement.^[1b,6,9] In general, the light-trapping problem in PeLED is caused by the high refractive index nature of perovskite materials,^[10] which makes the light escaping cone limited to a narrow-angle. Additionally, the high index of bulk perovskite also leads to low exciton binding energies.^[11] Moreover, the refractive index of a material is related to its bandgap.^[12] With the simple Moss relation

$$\frac{n^4}{\lambda_e} = 77 \mu\text{m}^{-1} \quad (3)$$

where n is the refractive index and λ_e is the wavelength corresponding to the absorption edge.^[12a,13] Therefore, for semiconductor light-emitting materials (emission wavelength $\approx 400\text{--}700$ nm), the refractive index will fall in the $n \approx 2.36\text{--}2.71$ range. But note that this is just the simplified situation, the refractive index relation with the bandgap can be more complicated. **Table 1** gives examples of refractive indexes of the three

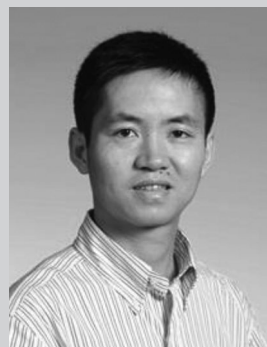


Qianpeng Zhang received his Ph.D. in ECE from HKUST in 2019. Currently, he is working with Prof. Zhiyong Fan at HKUST, as a postdoctoral scholar. Since 2015, he has been working on the fabrication of perovskite LEDs, the growth of perovskite nanowires, and the study on the related optical properties. His recent research focus

is on the light in-coupling and out-coupling behaviors in nanostructured perovskite devices.



Daquan Zhang is conducting postdoctoral research in the Department of ECE at HKUST. He achieved his Ph.D. degree in ECE from HKUST in 2020, and B.Eng. degree in Microelectronics from Wuhan University in 2014. His current research focus is on nanophotonics in perovskite nanowires/quantum wires, and their applications in optoelectronic devices.



Zhiyong Fan is a professor at the Department of Electronic and Computer Engineering, HKUST. He is a fellow of Royal Society of Chemistry and a founding member of The Hong Kong Young Academy of Sciences. His interests are on the design and fabrication of novel nanostructures and nanomaterials for high-performance optoelectronics, energy harvesting devices, and sensors.

Table 1. Bandgap and refractive index of some LED emission materials.

Material	Bandgap [eV]	Refractive index	Refs.
GaAs	1.43	$n \approx 3.3$	[24]
GaN	3.4	$n \approx 2.5$	[21,149]
TCTA:B3PYMPM: Ir(ppy) ₂ (acac)	2.6 (for Ir(ppy) ₂ (acac)) ^{a)}	$n_o = 1.83$, $n_e = 1.68$ (for undoped TCTA ^{b)} :B3PYMPM ^{c)} , and the modification by Ir(ppy) ₂ (acac) can be ignored when doping concentration is low)	[41a,68d,150]

^{a)}Ir(ppy)₂(acac): bis[2-(2-pyridinyl-N)phenyl-C](acetylacetonato)iridium(III); ^{b)}TCTA: [4,4',4''-tri(N-carbazolyl) triphenylamine]; ^{c)}B3PYMPM: [bis-4,6-(3,5-di-3-pyridylphenyl)-2-methylpyrimidine].

common light emitters, namely GaAs, GaN, and Ir(ppy)₂(acac). The former two are infrared and blue semiconductor emitters, and the latter one is the green organic emitter. According to Smith and Barnes,^[14] the typical index of the organic emitter is 1.7, which can be further reduced by using a low-index host (e.g., the index of polystyrene is 1.58). As a result, the index difference between the emission material and the air cannot be avoided. Therefore, the basic idea to improve the light OCE is to increase the light escaping angle, either by reducing the index difference between the emitter and air or by bringing in disturbance to the light-trapping effect. The index difference is more about the material choice and can be compromised by bringing in an index gradient.^[15] The disturbance to the light-trapping can be realized with varieties of nanophotonic engineering methods,^[16] which will be the focus of this review.

The light out-coupling in PeLEDs is more about the optics and photonics rather than materials themselves. Therefore, the experience gained on nanophotonics and nanoengineering can be potentially applied for the performance enhancement of PeLEDs.^[17] Although more and more researchers have started to work on the light out-coupling problem in PeLEDs,^[2a,9,10b,18] the number of reports on this topic is still limited. It is worth noting that, Yablonoitch,^[19] Friend^[20] and Nakamura,^[21] and their co-workers used to give very insightful discussions on the light out-coupling for GaAs LED, organic LED (OLED), and GaN LED, respectively, and a lot experience can be learned from them. Besides, there are also reports on the photon recycling and light out-coupling for PeLEDs from the PLQY point-of-view.^[6,8b,22] In this review, we would like to draw more attention to the topic of light out-coupling and provide useful hints for researchers to quickly set a course on this direction and further boost the performance of PeLEDs.

2. Photon Recycling

Friend, Snaith and co-workers reported the photon recycling (the re-absorption of radiatively recombining photogenerated charge pairs to regenerate an excitation) process in perovskites, and only 10–15% internally generated PL can escape to the air above or to the glass below for a thin film perovskite with the thickness about 100 nm.^[23] The remained emissions were guided in the film. By changing the substrate from flat

to textured one, the external PLQY was increased from 15% to 57%.^[23] Specifically, the radiative fraction of the recombination rate can be quantified by combining transient absorption (TA) measurement with transient PL measurement.^[6] Richter et al. found that PL was proportional to the radiative recombination rate, and TA was proportional to the carrier density.^[6] Moreover, the nonradiative recombination is not affected by the photon recycling because it does not provide photons. The light-emitting process is bimolecular, and the monomolecular nonradiative recombination is attributed to a trap-assisted Shockley–Read–Hall (SRH) recombination by Friend and co-workers.^[23] The photon recycling increases carrier concentrations in solar cells; as solar cells and LEDs are reciprocal, EQE of LEDs can be improved by texturing the substrate such as using microlens to suppress total internal reflection (TIR) and increase the refractive matching of the substrate.^[6] Figure 1a,b shows the photon recycling effect in the perovskite thin film.^[23] Figure 1c shows the external PLQY of perovskite thin film on different substrates.^[6] Note that photon recycling can help with the light out-coupling but is only efficient when the IQE of the active material is high.^[24]

3. The High Refractive Index of Perovskite

Löper et al. reported the refractive index of CH₃NH₃PbI₃ to be $n = 2.611$ at 633 nm, which was determined by spectroscopic ellipsometry and spectrophotometry.^[25] The refractive index is related to the band structure of the material and is used to describe the response of the material to light. Note that Green et al. have reviewed the optical properties of perovskite comprehensively.^[26] The optical properties are rigorously limited by nature,^[27] and Kramers–Kronig (KK) relationships give the fundamental connections. Moreover, the following formula is given to estimate the refractive index

$$n^2 - 1 = E_d E_0 / (E_0^2 - E^2) \quad (4)$$

This relationship was proposed by Wemple and Di Domenico.^[28] E is photon energy. E_d and E_0 are constants determined by selected chemical bonding and related material properties. With the above formula, Green and co-workers calculated the refractive indexes of MAPbI₃, MAPbBr₃, FAPbI₃

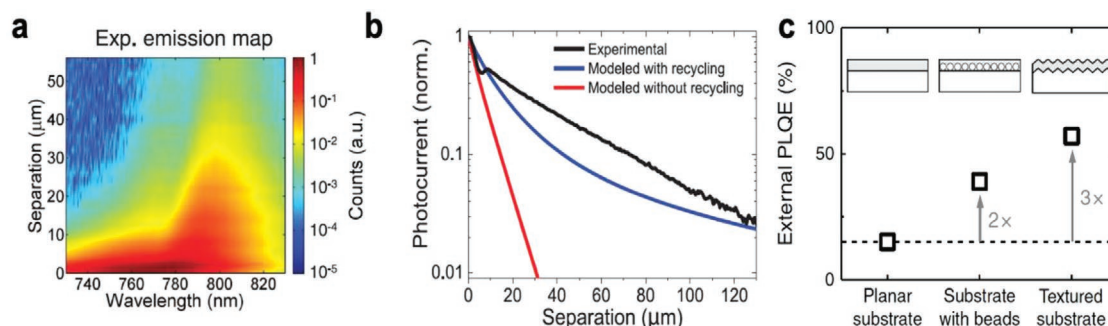


Figure 1. Photon recycling in perovskite thin film. a) Experimentally measured light emission map for different separation distances between excitation and collection. b) Predicted spatial photocurrent decay for the model with and without photon recycling. Reproduced with permission.^[23] Copyright 2016, AAAS. c) External PLQYs for MAPbI_{3-x}Cl_x on different substrates. Reproduced with permission.^[6] Copyright 2016, Springer Nature.

(FA means formamidinium), and FAPbBr₃ to be 2.5, 2.1, 2.5, and 2.1, respectively. Formula (4) can be further simplified as follows

$$n^2 \approx 1 + \frac{8.32 \text{ eV}}{E_g} \quad (5)$$

Intriguingly, according to Green and co-workers, one of the key optical features of organic-inorganic hybrid perovskite is the relatively low refractive index compared to traditional inorganic tetrahedrally coordinated semiconductors. Xie et al. also reported the characterization of the refractive index of MAPbI₃ and performed finite-difference time domain (FDTD) simulation with the acquired data for solar cells.^[29] Alias et al. reported the optical constant of MAPbBr₃, and obtained the dielectric function of 5.1 ($n \approx 2.26$) at the absorption edge.^[10a] Tauc-Lorentz (TL) optical dispersion model was used for the perovskite thin film. The information of the refractive indexes is important because it is required when designing the waveguiding or the light manipulation mechanism in perovskite-based optoelectronic devices.^[30] Huang and co-workers characterized the optical constants of continuous FAPbI₃ thin film for light out-coupling simulation.^[2a] Intriguingly, Stranks et al. mentioned that the dielectric function of perovskite could be affected by the photogeneration of carriers and likely the current injection, due to the soft and ionic nature of perovskite materials,^[1b,31] which means that the light out-coupling properties of PeLEDs are dynamic and can be very complicated.

4. The Progress on PeLED Performance

Figure 2 shows some of the representative works of the state-of-art PeLED devices. For the infrared and green light PeLEDs, Huang group and Wei group reported the $\approx 20\%$ EQEs at almost the same time in the year 2018, shown in Figure 2a–c and Figure 2d–f respectively.^[2a,c] Figure 2a is the diagram showing the device structure from Huang and co-workers. 5-aminovaleric acid (SAVA) modified FA perovskite was used as the emission material which formed the isolated sub-micrometer disks rather than a continuous film. Hence, the light out-coupling can be enhanced (from around 20% to more than 30%) due to the light scattering caused by the sub-micrometer structures. Figure 2b shows the EQE and energy conversion efficiency curves. The 20.7% peak EQE was achieved at 18 mA cm⁻² current density (electroluminescence (EL) peak at 803 nm, infrared color). Figure 2c shows the cross-sectional scanning transmission electron microscope (STEM) image. Micro-disks can be clearly resolved. The poly(9,9-dioctyl-fluorene-co-N-(4-butylphenyl) diphenylamine) (TFB) layer also shows pretty good coverage on top of the noncontinuous perovskite layer, which is important to avoid the current leakage.

Figure 2d is the diagram of the device structure in the work by Wei and co-workers. CH₃NH₃Br (MABr) was used to passivate CsPbBr₃ to form the quasi-core/shell structure. The MABr shell passivated the surface nonradiative defects and therefore boosted up the PLQY of the perovskite. 20.31% EQE was achieved for the green light at the luminance of 3400 cd m⁻² (emission peak at 525 nm), and the EQE curve is shown in

Figure 2e. Figure 2f is the STEM image that clearly shows the core/shell structure with the white arrows indicating the grain boundaries and MABr shells.

Later in 2018, Chiba et al. reported the red light PeLED with 21.3% EQE.^[2b] The red emission QDs were fabricated from pristine CsPbBr₃ using halide-anion containing alkyl ammonium (OAM-I) and aryl ammonium (An-HI) salts. Figure 3a is the energy diagram of the QDs LED (QLEDS). Figure 3b is the EQE curves, and OAM-I and An-HI QDs LEDs show the maximum EQEs of 21.3% and 14.1%, respectively, both at around 0.01 mA cm⁻². Figure 3c,d are the scanning electron microscopic (SEM) images of the OAM-I QDs and An-HI QDs, respectively.

In 2019, Jin and co-workers reported the highest EQE of 9.5% (at a luminance of 54 cd m⁻²) for blue LED at that time.^[3a] Figure 3e is the device energy diagram. Figure 3f is the EQE curve of the best device. Figure 3g is the STEM–high-angle annular dark-field (STEM–HAADF) image of the cross-sectional sample, showing the ultrathin perovskite layer with a quantum confinement effect. Very recently, Huang and co-workers reported sky-blue PeLEDs with 11% EQE by addressing the low PLQY problem in the wide bandgap perovskite with adding in the Yttrium (III) chloride, which broke the record for blue.^[3c] It is worth noting that blue PeLED is the key for building up micropixel LEDs, as pointed out by Halpert and co-workers in 2019.^[3b]

Last but not the least, it is worth more attention to standardizing measurement methods as more and more high-efficiency PeLEDs are being reported rapidly.^[32] Recently, Stranks and co-workers proposed a few standards for the characterization and comparison of PeLED devices,^[33] which can largely benefit the community. More measurement standards can also be found from the references by Snaith, Friend, and Forrest respectively.^[34]

5. Light Out-Coupling Strategies for LEDs

From the above introduction and discussions, we know that the IQE of PeLEDs is already high, and the EQE has almost reached the upper limit unless the light out-coupling strategies are deployed. Therefore, in this section, we will first review the current progress on the light out-coupling studies for PeLEDs and then look at the successful light out-coupling strategies for OLEDs, conventional semiconductor LEDs, QDs and multiple quantum wells (MQWs) LEDs, etc., in order to acquire more inspiration. Moreover, we will also discuss the special LEDs such as nanowire LEDs. Last, we will review the simulation methods for PeLEDs for the light out-coupling study. By learning from the successful strategies for LEDs based on other materials, hopefully, we can deliver useful hints for further development in PeLEDs.

5.1. Light Out-Coupling for PeLEDs

Recently, there are a few reports on improving perovskite LED performance with light out-coupling strategies. Tang and co-workers performed the systematic theoretical simulations

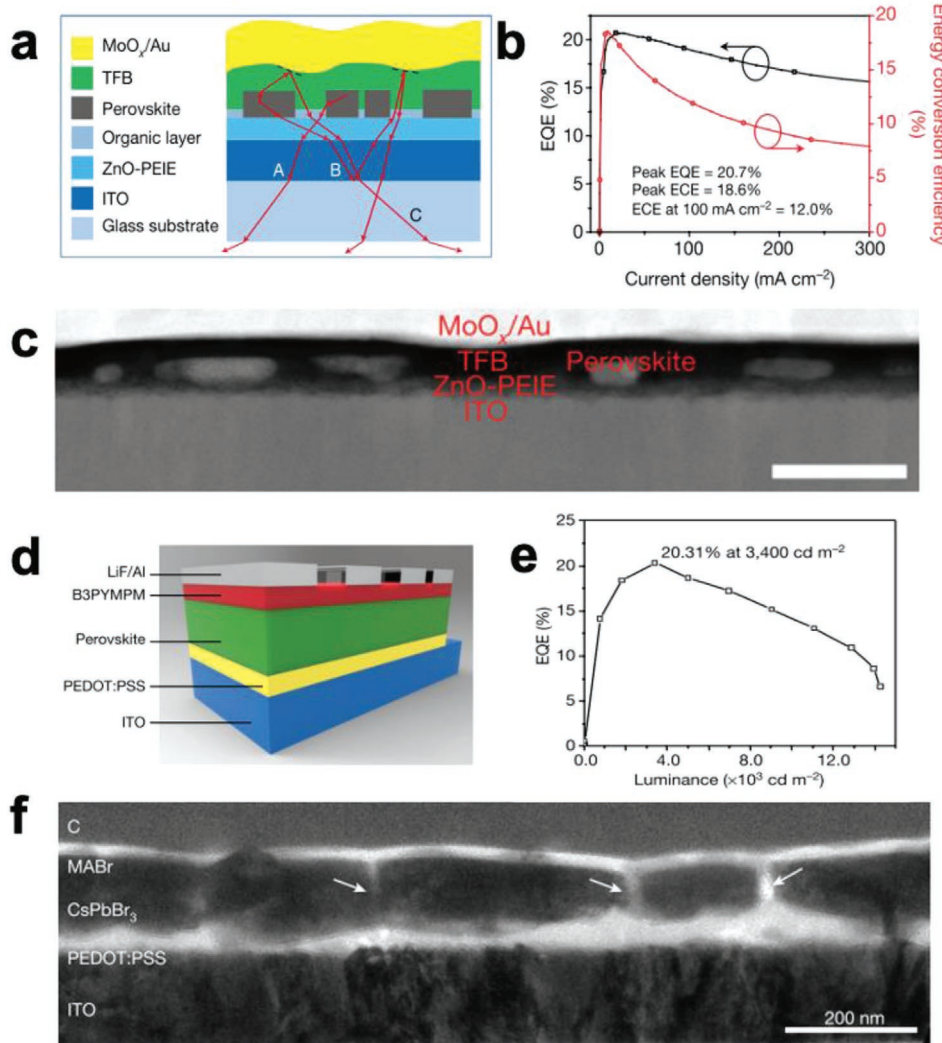


Figure 2. Progress of the state-of-art perovskite LED devices (I). a–c) NIR perovskite (5AVA:FAPbI₃) LEDs with 20.7% EQE. (5AVA, 5-aminovaleric acid) a) Device structure diagram. Perovskite layer has spontaneously formed sub-micrometer structures. b) EQE curve and energy conversion efficiency curve. The maximum EQE of 20.2% was achieved at 18 mA cm⁻². c) Cross-sectional STEM image showing the complete device with the sub-micrometer structures. The scale bar is 200 nm. Reproduced with permission.^[2a] Copyright 2018, Springer Nature. d–f) Green perovskite (quasi-core/shell MABr: CsPbBr₃) LEDs with 20.3% EQE. d) The diagram showing the device structure. e) EQE spectrum. The maximum EQE is 20.3% at 3400 cd m⁻². f) Cross-sectional TEM image showing the quasi-core/shell perovskite on the PEDOT:PSS. The white arrows show the MABr shell. Reproduced with permission.^[2c] Copyright 2018, Springer Nature.

to discuss the correlation between OCE and several key factors such as the refractive index differences, the layer thicknesses, and the emitter dipole orientations.^[18c] Moreover, Gao and co-workers simulated and demonstrated how the large reflective index influenced the optical loss in both 3D and quasi-2D perovskite material systems.^[35] The results revealed that after device engineering, the maximum EQEs for 3D and quasi-2D PeLEDs can theoretically reach 25% and 20%, respectively. For 3D PeLEDs, the thickness of the emission layer affects both light out-coupling and charge injection, therefore the balance between these two factors needs to be considered when tuning the thickness. However, for quasi-2D PeLEDs, the thickness of the emission layer almost has no effect on the OCE. As a result, charge injection becomes a major concern for thickness optimization of quasi-2D PeLEDs.

More importantly, experimental works focusing on the design of nanophotonic structures for high OCE PeLEDs were also reported. Fan and co-workers fabricated the efficient MAPbBr₃ PeLEDs onto the nanophotonic substrate that was comprised of the nanodome light coupler and the nanowire arrays optical antennas (Figure 4a).^[10b] The EQE was enhanced from 8.19% to 17.5% with the optimized nanophotonic substrate (Figure 4b). Besides, anodic alumina membrane (AAM) substrates with various pore diameter/pitch (D/P) ratios were studied. After the nanopores were filled with high refractive index TiO₂ ($n_{\text{TiO}_2} = 2.6$, $n_{\text{Al}_2\text{O}_3} = 1.7$), the TiO₂ nanowires together with AAM play a role as a positive photonic crystal and it can work as the optical antennas with proper geometry. The light OCE of P500, P1000, and P1500 devices were 5.2%, 73.6%, and 26.9%, respectively. Based on FDTD simulations, the photonic crystal optical

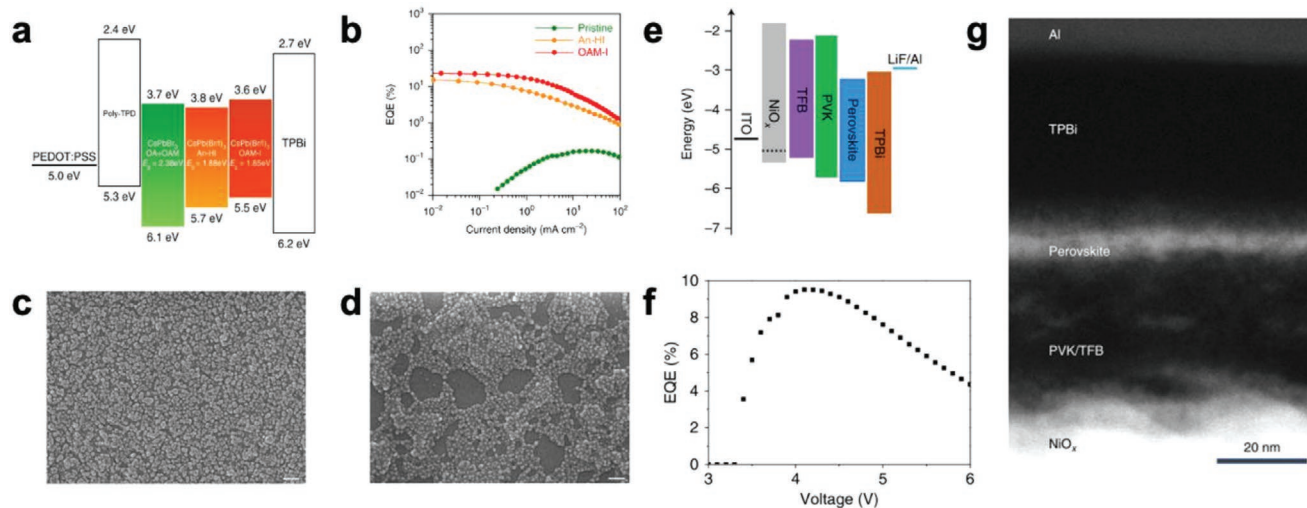


Figure 3. Progress of the state-of-art perovskite LED devices (II). a–d) Red perovskite (pristine CsPbBr₃ perovskite QDs using long alkyl ammonium and aryl ammonium. OAM-I, alkyl ammonium; An-HI, aryl ammonium.) LED with 21.3% EQE. a) Energy diagram of the perovskite QDs LEDs. b) EQE versus current density (EQE–*J*) curves. OAM-I and An-HI QDs LEDs show the maximum EQEs of 21.3% and 14.1% respectively, both at around 0.01 mA cm⁻². SEM images of c) OAM-I QDs and d) An-HI QDs. Reproduced with permission.^[2b] Copyright 2018, Springer Nature. e–g) Blue perovskite (quasi-2D Cs_xFA_{1-x}PbBr₃ nanoparticles) LEDs with 9.5% EQE. e) The energy band diagram of the device. f) The EQE curve versus voltage. The maximum EQE of 9.5% was achieved at 54 cd m⁻². g) The STEM–high-angle annular dark-field (STEM–HAADF) image of the cross-sectional sample. Reproduced with permission. Copyright 2019,^[3a] Springer Nature.

antennas can convert guided modes (or waveguide modes) to leaky modes and lead to the enhanced light out-coupling in the nanostructured device (Figure 4c).

Meanwhile, Tang and co-workers demonstrated the moth-eye nanostructured ZnO layer for PeLEDs.^[18d] The patterned ZnO layer was used as not only the hole-injection layer but also an out-coupling layer to extract the waveguide modes (Figure 5a). The corrugated nanostructures and compact contacts between each layer can be clearly resolved from the cross-sectional SEM image of the complete device (Figure 5b). With the out-coupling structure at the front electrode/perovskite interface, most of the trapped light was scattered out, leading to enhanced light emission. Moreover, the broadband total transmittance enhancement was attributed to the gradient refractive index of the moth-eye nanostructures (Figure 5c). Therefore, the green-light PeLEDs with the light out-coupling structure showed the EQE of 20.3% and the current efficiency (CE) of 61.9 cd A⁻¹, with 1.5 times-enhancement compared to the planar counterparts. More intriguingly, the EQE and CE were further enhanced to 28.2% and 88.7 cd A⁻¹ respectively, after applying the half-ball lens. As far as we know, the 28.2% EQE is the highest reported value for PeLEDs until now (Figure 5d).

Rand and co-workers showed that the perovskite layer thickness is critical for both the efficiency and the stability of PeLEDs.^[18b] The device structure is shown in Figure 6a. Moreover, the optimized thickness of the perovskite layer was in the range of 35–40 nm for different perovskite compositions. The maximum EQEs were 17.6%, 14.3%, 11.3%, and 10.1% for Cs_{0.2}FA_{0.8}PbI_{2.8}Br_{0.2}, MAPbI₃, FAPbBr₃, and FAPbI₃ PeLEDs respectively (Figure 6b–e). The thin-emission layer reduces the waveguide mode loss. Additionally, the thin emission layer also contributed to the enhanced stability by reducing the Joule heating.

Jeon et al. demonstrated the PeLEDs with improved OCE by using the nanohole array (NHA) embedded in the SiN layer between indium tin oxide (ITO) and glass (Figure 7a).^[18a] The high refractive index contrast between voids ($n = 1.0$) and SiN ($n = 2.02$) help to couple out the waveguide modes and substrate modes. Moreover, the PeLEDs with NHA showed 1.64-times higher EQE (from 8.9% to 14.6%) than PeLEDs without NHA structure (Figure 7b). The *E*-field intensity distributions with NHA structure are shown in Figure 7c,d. Clearly, the *E*-field intensity is significantly proliferated with NHA structure and more light can enter the glass substrate. Especially, the far-field intensity (Figure 7e) can be deduced from the *E*-field distribution in glass substrate by the plane wave expansion method.^[36] The far-field intensities can show a clear comparison of the OCEs from different substrates.

Different from the above-mentioned methods which apply nanostructures/patterns outside the emission layer, Huang and co-workers used molecular engineering and directly formed micro-structures inside the perovskite layer, as previously shown in Figure 2a–c.^[2a] Note that the concentration of the 5AVA-FAPbI₃ precursor solution needs to be optimized. Otherwise, either OCE will be sacrificed in high coverage perovskite film (for high concentration) or the leakage current will be severe (for low concentration).

Special attention should be paid to a very enlightening work reported by Di, Friend, and co-workers.^[37] The 20.1% EQE was achieved from the perovskite–polymer bulk heterojunction (PPBH) LEDs. They mentioned that the index of PPBH system ($n \approx 1.9$) is much lower than that of the perovskite material ($n \approx 2.7$), therefore the lower index can widen the photon escape cone to 32° and meanwhile achieve an OCE of 21%. Another very important strategy is to reduce the refractive index of perovskite material by mixing with other additives such as large

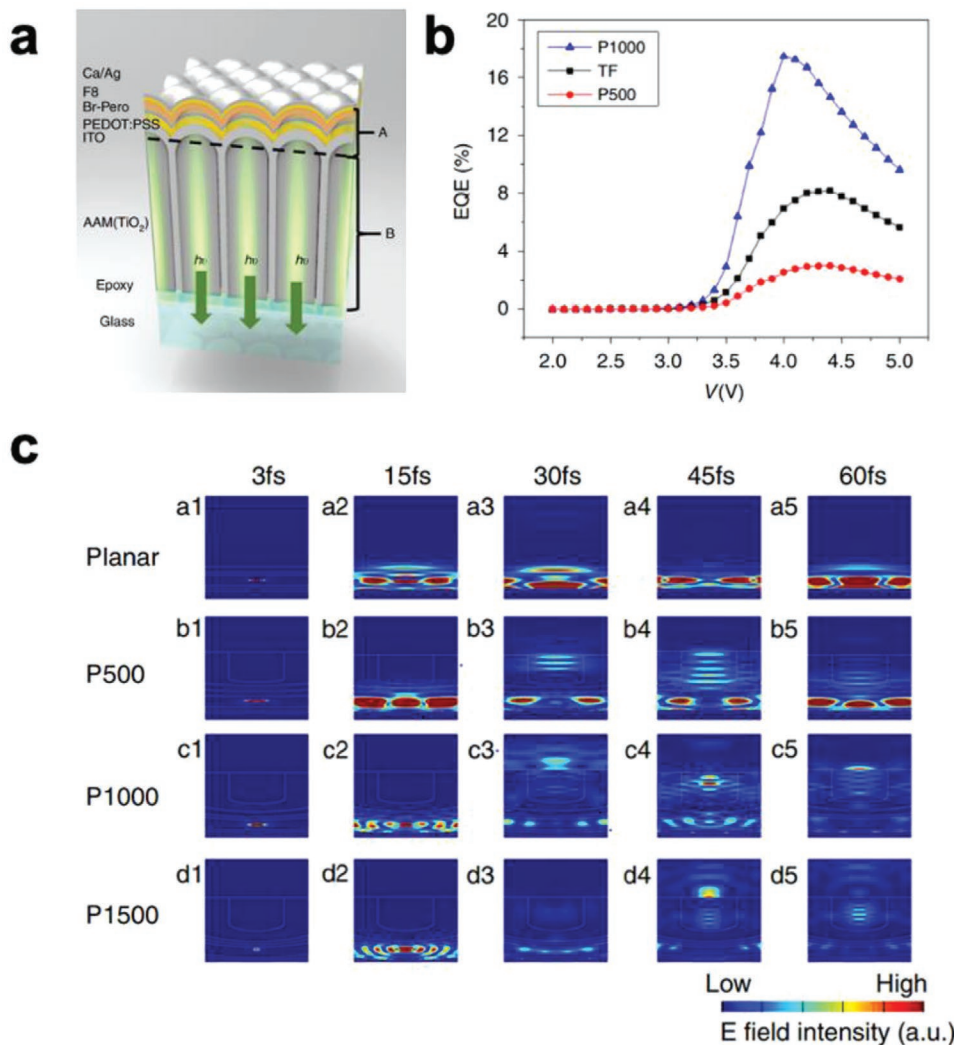


Figure 4. Out-coupling improvements in perovskite LEDs (I). a–c) TiO₂ nanowire arrays embedded in AAM working as 3D nanophotonic substrates to enhance light extraction. a) Schematic of the device on the nanophotonic substrate. The device structure from bottom to top is AAM with TiO₂ filled in channels, ITO, PEDOT: PSS, green light perovskite, F8, and Ca/Ag electrode. b) EQE curves of the thin film device and devices with the nanophotonic substrates. c) *E* field change for different structures (from top to bottom: planar, P500, P1000, and P1500, P means pitch here) at different timescale (from left to right: 3, 15, 30, 45, and 60 fs). Reproduced with permission.^[10b] Copyright 2019, Springer Nature.

amount of organic cations (e.g., MAI, MABr) or other organic components.^[2a,18a,35]

Table 2 summarizes the works that have discussed the light out-coupling (or light extraction) for PeLEDs.

5.2. Light Out-Coupling For Organic LEDs

As PeLEDs and OLEDs have a lot of aspects (e.g., device structure, injection materials, fabrication processes, etc.) in common, studying the light out-coupling strategies that have been proved to be successful in OLEDs can save a lot of efforts for PeLEDs researchers. OLEDs have attracted a lot interests since the EL was first reported in anthracene crystals by Helfrich and Schneider in 1965.^[38] More significantly, the first OLED device was reported by Tang and VanSlyke in 1987.^[39] Compared with conventional LEDs, OLEDs are more promising

in flat panel display and illumination applications because of the more efficient radiative recombination in organic active materials.^[40] Note that near 100% IQE has been achieved in OLEDs.^[41] However, there is still a bottleneck for OLEDs due to the limited OCE. Specifically, in conventional planar OLEDs, there is more than 80% light loss through the waveguide mode, substrate mode, electrode absorption and the surface plasmons, as discussed by Smith et al.^[42] Significant progress has been made to improve the OCE in both bottom-emission and top-emission OLEDs, from which we can also learn some light out-coupling strategies for PeLEDs.

5.2.1. Approaches for Enhancing OCE in Bottom-Emission OLEDs

In a bottom-emission device, the light is coupled out through a transparent bottom electrode which is usually the ITO/glass

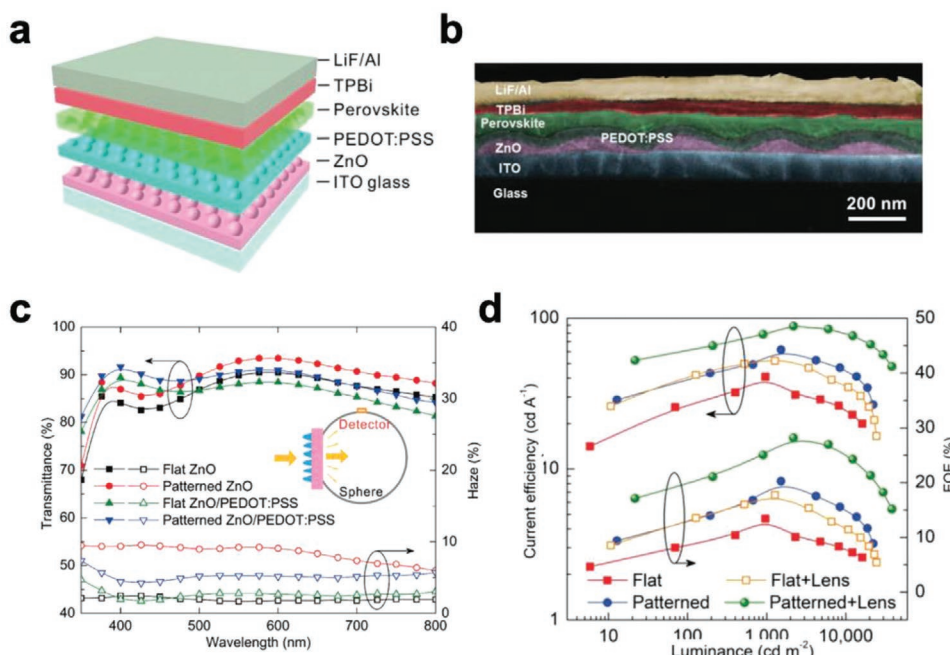


Figure 5. Out-coupling improvements in perovskite LEDs (II). a–d) Moth-eye nanostructures at the ITO/perovskite interface to improve the OCE of PeLEDs. a) The device structure of CsPbBr₃ PeLEDs with the imprinted nanostructures. b) Cross-sectional SEM image of the device with patterned ZnO layer. c) Optical transmission and haze spectra of flat and patterned substrates. d) Current efficiency (CE) and EQE of flat and patterned PeLEDs as a function of luminance. Reproduced with permission.^[18d] Copyright 2019, Wiley-VCH.

substrate. Considering the large differences between the refractive index of different layers ($n_{\text{organic}} \approx 1.7\text{--}2.0$, $n_{\text{ITO}} \approx 1.8$, $n_{\text{glass}} \approx 1.45$, $n_{\text{air}} = 1.0$), most of the emitted light is trapped as the waveguide mode and substrate mode.^[43] Typically there are two techniques

for improving the light OCE in bottom-emission OLEDs. The first one is employing an extra scattering layer to couple out the waveguide modes. Gu et al. demonstrated the utilization of a layer of Pt-Co alloy nanoparticles (NPs) as a buffer layer

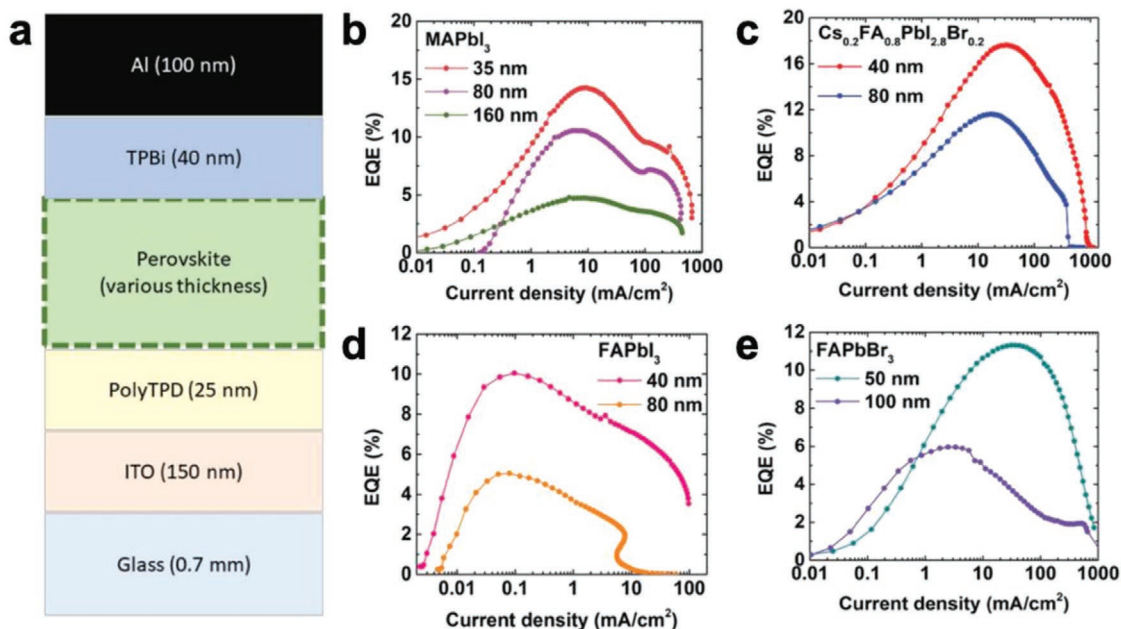


Figure 6. Out-coupling improvements in perovskite LEDs (III). a–e) Perovskite layer thickness optimization to improve light out-coupling. a) The device structure of PeLEDs with various thicknesses and different chemical compositions. b–e) EQE of perovskite emission layer based on: b) MAPbI₃, c) Cs_{0.2}FA_{0.8}PbI_{2.8}Br_{0.2}, d) FAPbI₃, and e) FAPbBr₃ with different optimal perovskite thicknesses. Reproduced with permission.^[18b] Copyright 2018, Wiley-VCH.

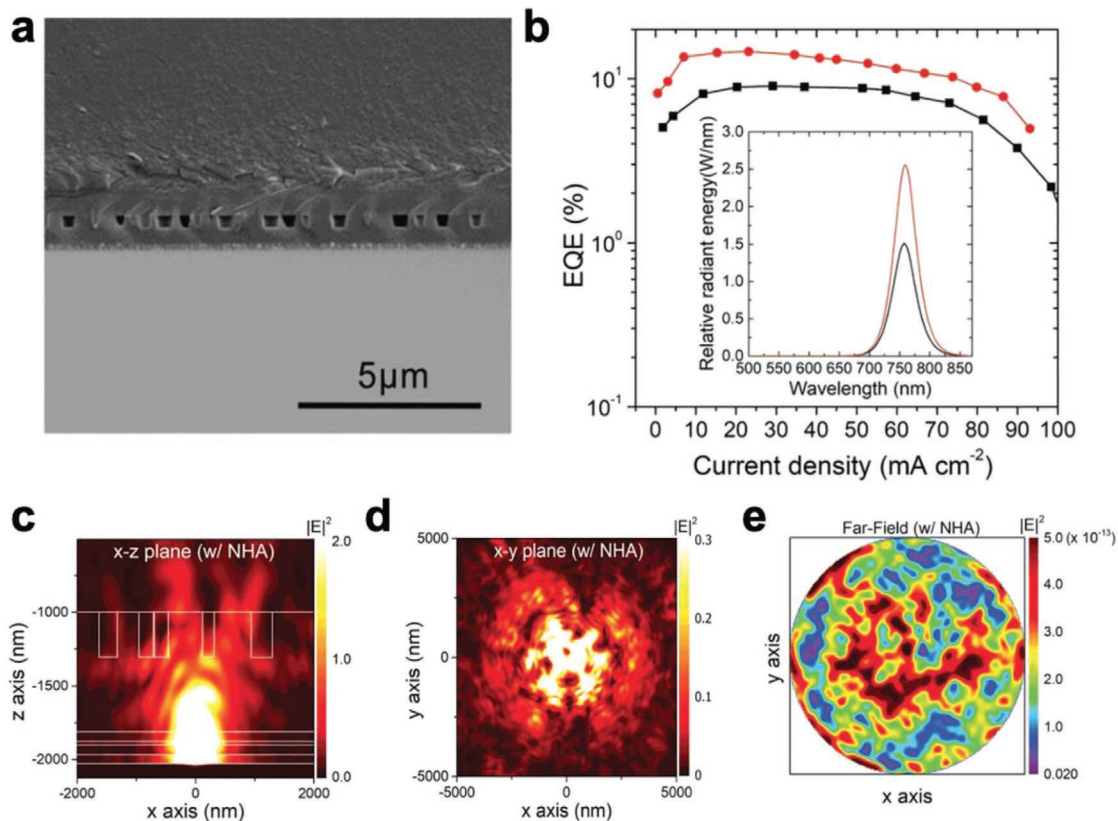


Figure 7. Out-coupling improvements in perovskite LEDs (IV). a–e) Randomly distributed nanohole array with high refractive index contrast to increase out-coupling efficiency in PeLEDs. a) SEM image of nanohole array (NHAs) structure utilized in improved out-coupling PeLEDs. b) EQE versus current density curves of PeLEDs with and without NHAs. The inset displays the relative radiant energy spectra. The *E*-field intensity distribution of PeLEDs with NHAs in c) cross-sectional view (in *x*–*z* plane) and d) top view (in *x*–*y* plane). e) The far-field intensity of PeLEDs distribution with NHAs outside the glass substrate at 1 m distance from the glass/air interface. Reproduced with permission.^[18a] Copyright 2019, Wiley-VCH.

Table 2. The OCEs and the light out-coupling methods of PeLEDs.

Ref.	Materials (color)	External quantum efficiency (EQE)	Current efficiency (CE)	OCE	Enhancement	Light out-coupling methods
[2a]	5AVA/FAI/PbI ₂ (infrared)	20.7% (at 18 mA cm ⁻²)	N.A.	More than 25% (over 310–900 nm range)	OCE from less than 20% to more than 25%	Spontaneously formed sub-micrometer-scale structures
[18d]	CsPbBr ₃ (green)	28.2%	88.7 cd A ⁻¹	N.A.	N.A.	Bio-inspired moth-eye nanostructures, and half-ball lens
[10b]	BABr:MAPbBr ₃ (green)	17.5% (at 4.0 V)	N.A.	73.6%	EQE from 8.19% to 17.50%; OCE (or light extraction efficiency) from 10% to 73.6%	Nanodome light coupler + nanowire optical antennas
[18b]	Cs _{0.2} FA _{0.8} PbI _{2.8} Br _{0.2} (infrared); MAPbI ₃ (infrared); FAPbI ₃ (infrared); and FAPbBr ₃ (green)	17.6% (for Cs _{0.2} FA _{0.8} PbI _{2.8} Br _{0.2}); 14.5% (for MAPbI ₃); 10.1% (for FAPbI ₃); and 11.3% (for FAPbBr ₃)	N.A.	≈15% (for MAPbI ₃ with ≈40 nm thickness)	N.A.	Thin emission layers
[119]	MABr:CsPbBr ₃ (green)	16%	N.A.	40–50%	EQE from 11% to 16%; OCE from 10–20% to 40–50%	Perovskite nanowires
[18a]	MAPbI ₃ (infrared)	14.6% (at ≈7 mA cm ⁻²)	N.A.	N.A.	EQE enhanced 1.6 times (from 8.9% to 14.6%)	Nanohole array

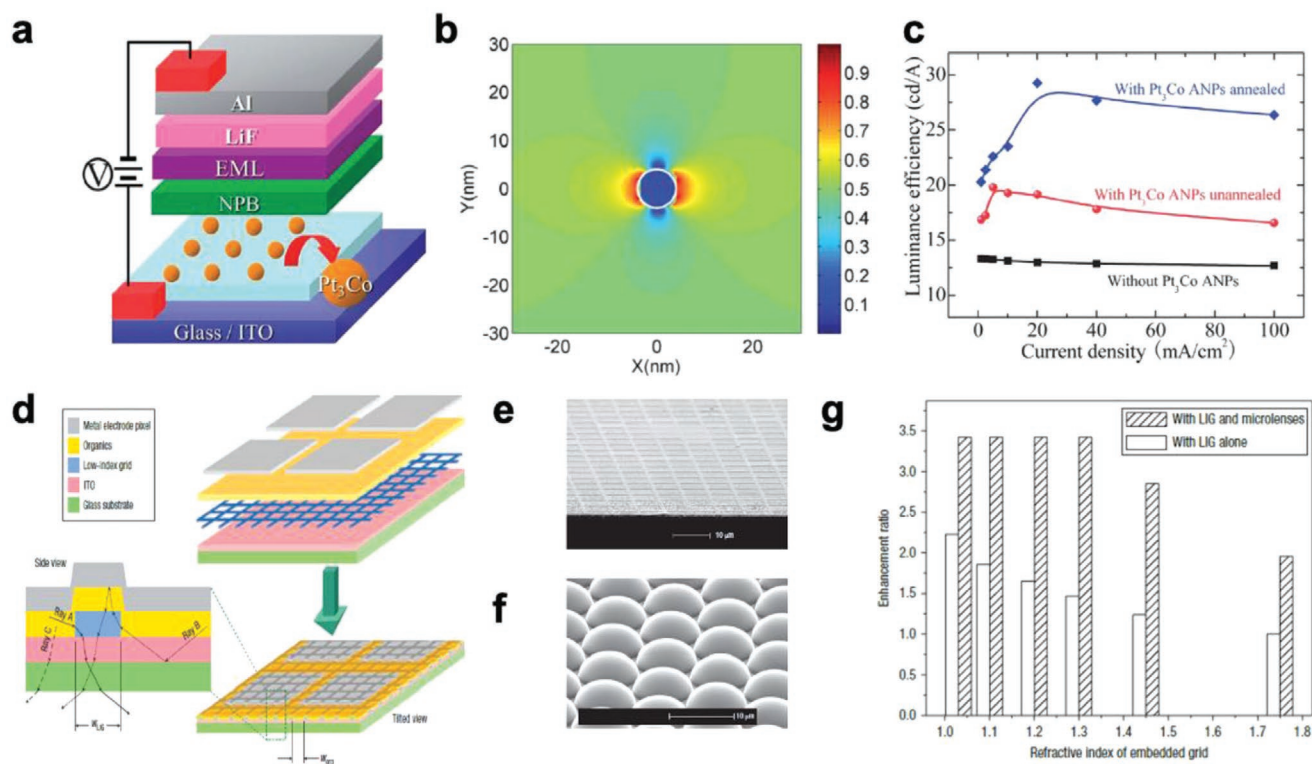


Figure 8. Strategies for light out-coupling enhancement in bottom-emission OLEDs (I). a–c) Localized surface plasmonic and light-scattering effect for light out-coupling enhancement: a) Schematic of the device with Pt₃Co nanoparticles on the ITO substrate. b) Normalized electromagnetic field distribution around a single Pt₃Co nanoparticle with a diameter of 8 nm. c) Device performance comparison. Reproduced with permission.^[44] Copyright 2013, The Royal Society of Chemistry. d–g) Embedded low-index grid for light out-coupling enhancement: d) Schematic demonstration of the OLEDs with embedded low-index grid. The SEM images of e) the grid and f) hexagonal arrays of hemispherical polymer microlenses. g) Simulated enhancement ratio of the light out-coupling efficiency (OCE) with different refractive index grids. Reproduced with permission.^[46] Copyright 2008, Springer Nature.

to enhance both the IQE and OCE.^[44] As shown in **Figure 8a**, a layer of Pt-Co NPs was incorporated between the ITO and organic hole transport layer (HTL) via spin-coating and post-annealing. **Figure 8b** shows the calculated distribution of normalized electromagnetic (EM) field around a single Pt₃Co NP with a diameter of 8 nm. The EM wavelength for calculation was the same with the EL peak position (530 nm). The near-field was enhanced in the *x* (polarization) direction but reduced in the *y* (light incident) direction, which could be attributed to the NPs-induced localized surface plasmon (LSP) and light-scattering effects, respectively. Both two effects increase the out-coupling of the waveguide modes. Meanwhile, the strong resonance between the exciton and LSP increases the total number of excitons generated in the organic emission layer and hence improves the IQE of the device.^[45] **Figure 8c** shows the luminance efficiency-current density curves for different devices. Compared with the conventional device without Pt-Co NPs, there was more than 100% enhancement in the luminance efficiency of the device with Pt-Co NPs (without annealing). Moreover, the post-annealing of Pt-Co NPs increased the surface roughness and further enhanced the light scattering effect and the OCE. Consequently, there was around 50% luminance efficiency improvement with annealing, as shown in **Figure 8c**.

Moreover, the low-index-grid (LIG) was embedded in the OLED active layer to improve the light OCE, as reported by Sun and Forrest.^[46] The schematic device structure and the grid

SEM images are shown in **Figure 8d–f**, respectively. The period of the grid was about ten times the wavelength. Moreover, the high-angle modes (Ray A and B in **Figure 8d**) normally trapped by the TIR can be refracted toward the substrate normal, when passing through the low index region. As a result, the OCE was enhanced by 2.3 ± 0.2 times, compared to the conventional device without LIG. To further improve the OCE, the array of microlens was applied for the out-coupling of the substrate mode, as shown in **Figure 8f**. Moreover, the OCE enhancement ratio as a function of the grid material index is plotted and shown in **Figure 8g**. It is worth mentioning that, the low-index material used was aerogel with the index $n = 1.03$.^[47] However, when the LIG layer was within the active layer, the undesired modification to the emission material can introduce rough internal interfaces and current shorts.^[46,48] To address this problem, the same group inserted the sub-anode planar grid layer between ITO and glass for efficient substrate mode out-coupling.^[49] The OLEDs device and grid structures are schematically shown in **Figure 9a**. The grid consists of two transparent materials with different refractive indexes. Because the grid layer is outside the active region, the device fabrication and operation are not affected by the grid, therefore the performance can be separately optimized for the extra out-coupling layer and the device. Using the photonic crystals is another effective approach to improve the OCE.^[16b,50] For example, Do et al. demonstrated 2D SiO₂/SiN_x photonic crystals between

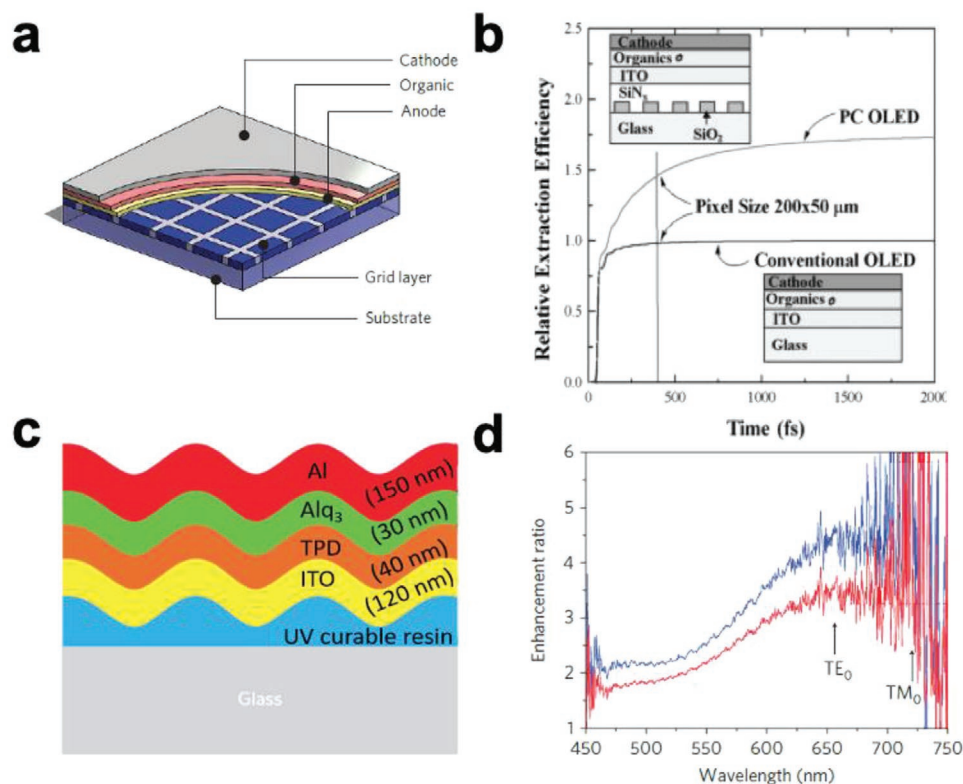


Figure 9. Strategies for light out-coupling enhancement in bottom-emission OLEDs (II). a) Sub-anode grids for light out-coupling enhancement: Schematic of the device structure. Reproduced with permission.^[49] Copyright 2015, Springer Nature. b) Relative light OCE of OLEDs with and without 2D SiO₂/SiN_x photonic crystal patterns with the device diagram inserted. Reproduced with permission.^[50e] Copyright 2003, Wiley-VCH. c,d) Spontaneously formed buckling pattern for light extraction: c) schematic of the OLED device with buckles. d) Enhancement ratio of intensity by buckling as a function of emission wavelength. Reproduced with permission.^[48b] Copyright 2010, Springer Nature.

ITO and glass substrate to achieve a significant OCE improvement, as shown in Figure 9b.^[50e] From the FDTD simulation result, the maximum OCE was increased more than twice. The optimized photonic crystals had a lattice constant of 600 nm, a diameter of 480 nm, and a height of 300 nm.

Although the above-mentioned out-coupling layer can bring in significant OCE enhancement, it is sensitive to the wavelength and the structure geometry, which severely limits the applications in white light OLEDs. To address this issue, Koo et al. demonstrated a spontaneously formed buckling pattern for out-coupling waveguide modes over a broad wavelength range.^[48b] The device structure is shown in Figure 9c. The buckling patterns were produced by the thermal evaporation of ultrathin aluminum films (10 nm) on poly(dimethylsiloxane) (PDMS) substrate. Figure 9d shows the EL intensity enhancement ratio versus emission wavelengths. The EL intensity was enhanced by a factor of 1.8, 2.2, and more than 4 at 475 nm (blue), 525 nm (green), and 655 nm (red) respectively. As a result, the whole spectra in OLED can be well out-coupled with just one grating structure.

As most of the current PeLEDs are also bottom-emission type, adding a layer of NPs, a grid, a grating, or a buckling pattern into the ITO/glass interface can be possible effective methods to convert waveguide modes to the substrate modes. Moreover, hemispheres/nanowires can be added to the glass surface for further out-coupling of the substrate modes.

5.2.2. Approaches for Enhancing OCE in Top-Emission OLEDs

Even though research interests are focused on the bottom-emission OLEDs, top-emission OLEDs are more promising for active-matrix flat panel display as they emit light away from the substrate and the backplane circuit and increase the aperture ratio of the display.^[51] In the top-emission configuration, the light is coupled out via the top electrode, therefore using the high transparency electrode becomes one of the most effective ways for improving OCE.

For example, Meyer et al. applied the transparent Al-doped ZnO (AZO) electrodes for light out-coupling (Figure 10a).^[52] The AZO electrode was deposited by atomic layer deposition (ALD) and pulsed laser deposition (PLD) with a WO₃ buffer layer. The transmittance of the electrode is above 73% in the visible range. Finally, power efficiency and current efficiency of 27 lm W⁻¹ and 43 cd A⁻¹ were achieved in this top-emission OLED respectively.

Semitransparent Ca/Ag double-layer cathode was also reported by Lee et al. to achieve high OCE for top-emission OLEDs.^[53] Figure 10b shows the wavelength-dependent transmittance of the Ca/Ag double-layer cathode with different thicknesses. The optimum uniform transmittance (~80%) can be achieved in Ca (10 nm)/Ag (10 nm) structure. Han et al. demonstrated similar multilayer transparent top electrodes as both light out-coupling layer and buffer layer against radiation

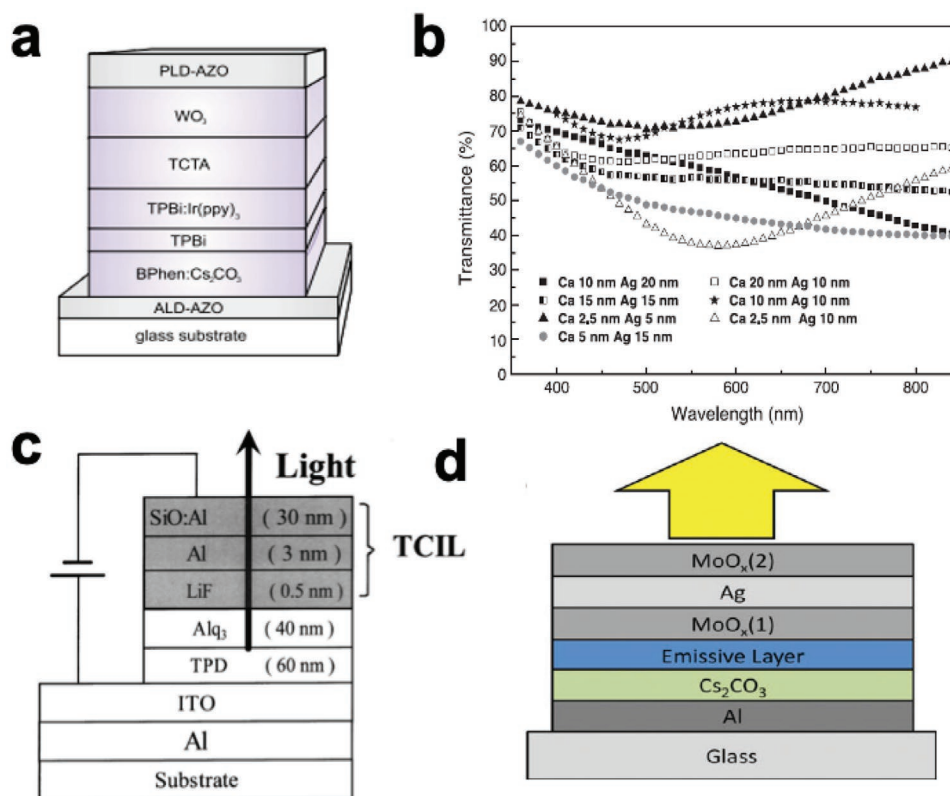


Figure 10. Strategies for light out-coupling enhancement in top-emission OLEDs (I). a) Schematic of a top-emission OLED using the AZO electrode. Reproduced with permission.^[52] Copyright 2008, American Institute of Physics. b) Transmittance spectra of the Ca/Ag double-metal layer with different thicknesses. Reproduced with permission.^[53] Copyright 2004, Elsevier. c) Schematic of a top-emission OLED using LiF/Al/Al-doped SiO as a transparent electrode. Reproduced with permission.^[54] Copyright 2003, American Institute of Physics. d) Schematic of the top-emission OLEDs with transparent MoO_x/Ag/MoO_x electrodes for light out-coupling enhancement. Reproduced with permission.^[55] Copyright 2014, Wiley-VCH.

damages from the following radio frequency (RF) sputtering processes.^[54] The device had a structure of LiF/Al/Al:SiO, as shown in Figure 10c.

Similarly, Yambem et al. reported the utilization of three-layer transparent MoO_x (5 nm)/Ag (10 nm)/MoO_x (40 nm) (MAMs) stack to improve the OCE.^[55] The device structure is shown in Figure 10d. The transmittance of such MAMs is around ≈75% at the peak, while the sheet resistance is below 10 Ω □⁻¹, even lower than that of some commercial ITO glasses. Moreover, the OCE of MAMs-based top-emission OLEDs is higher than the ITO-based bottom-emission OLEDs, which can be attributed to the refractive index differences in the three layers and the microcavity effect.^[56] At higher brightness, there was an average of 1.8- and a maximum of 2.1-times improvements in the current efficiency when the top-emission was used. Meanwhile, another advantage of the MAMs-based top-emission OLEDs is that the color remains unchanged at different viewing angles, while the color change is a common problem for many other OCE improvement strategies.^[57]

Moreover, WO₃/Ag/WO₃ multilayer transparent electrode has also been reported by Hong et al. for the top-emission OLEDs.^[58] As shown in Figure 11a, the optimized WO₃(30 nm)/Ag (12 nm)/WO₃(30 nm) stack can have a high transmittance of 93.8% and a low sheet resistance of 7.22 Ω □⁻¹. A thin layer high index WO₃ ($n > 2$) can fulfill the optimum zero-reflection condition

with a Ag metal layer. Figure 11b shows the EL performance of the devices with the WO₃/Ag/WO₃ electrode and with a single layer of 10 nm Al, respectively. When changing the pure Al electrode to the multilayer stack, the maximum luminance value (at $J = 220 \text{ mA cm}^{-2}$) was increased from 8400 to 11700 cd m⁻², and the power efficiency was increased by about 26%.

Hobson et al. reported that up to 40% of light loss could be attributed to the surface plasmon (SP) modes in a typical bottom-emission OLEDs.^[42b] Nevertheless, the situation is even worse for the top-emission OLEDs.^[59] Therefore, the recovery of the loss to the SP modes is of significant importance. Wang et al. demonstrated the nanoaggregated bathocuproine (BCP) film on top of a conventional top-emission OLEDs for OCE improvement.^[60] Figure 11c demonstrates the atomic force microscope (AFM) image of the nanoaggregated BCP film on Ag where a rough surface with a maximum vertical distance of 31.2 nm can be resolved. Furthermore, the device structure and EL intensity enhancement are shown in Figure 11d. There was an obvious EL intensity improvement by a factor of 2.1 to 2.7, compared with the planar counterparts.

Meanwhile, microstructures with the pitch at the wavelength scale are also effective in reducing the SP mode loss.^[61] Wedge et al. demonstrated a photoresist (PR) microstructure with a period of 338 nm on the planar metal electrode to out-couple the waveguide modes and SP modes to air.^[62] The device structure is schematically shown in Figure 11e. The PR

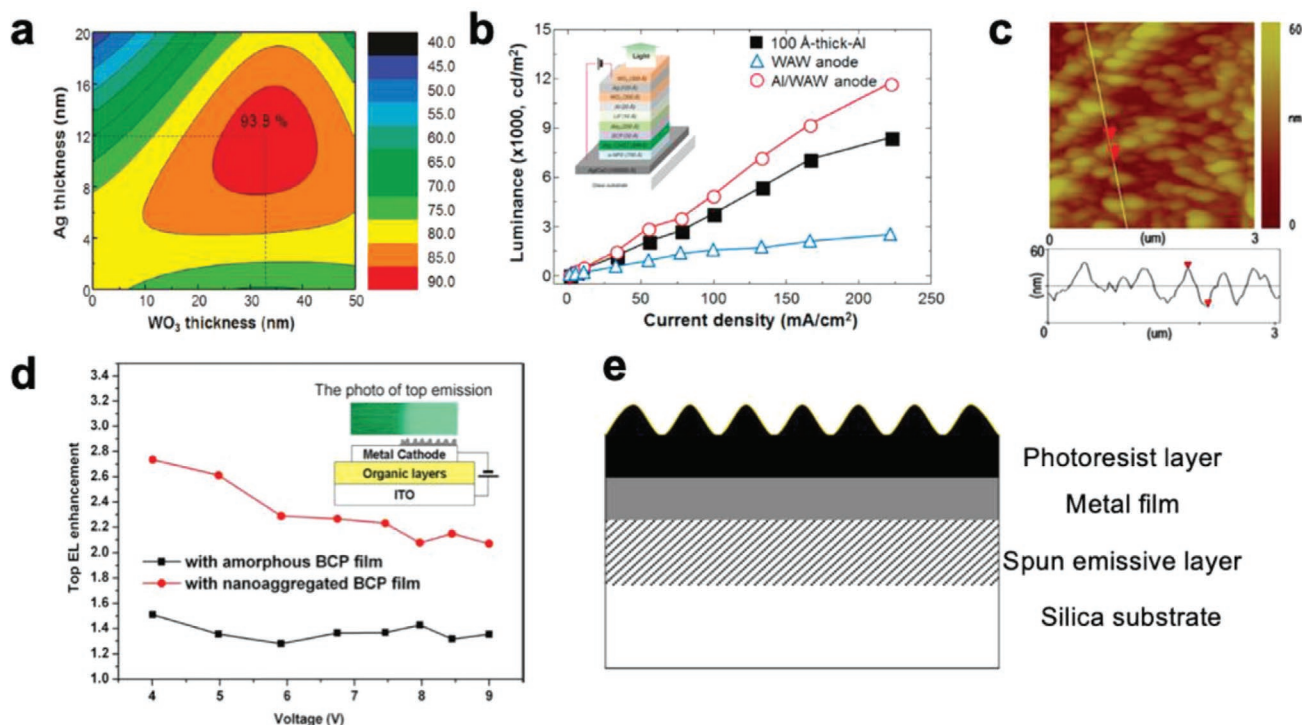


Figure 11. Strategies for light out-coupling enhancement in top-emission OLEDs (II). a,b) Transparent WO₃/Ag/WO₃ electrodes for light out-coupling enhancement: a) contour plot of the transmittance for the WO₃/Ag/WO₃ structure, and b) current density-dependent luminance of the top-emission OLEDs with single Al layer and WO₃/Al/WO₃ structure as top electrodes. The inset is the device diagram. Reproduced with permission.^[58] Copyright 2011, American Chemical Society. c,d) Nanoaggregated out-coupling layer for top-emission OLEDs light extraction enhancement: c) an AFM image of the nanoaggregated film on Ag film. d) Bias voltage-dependent EL intensities of a top-emission OLED with and without nanoaggregated out-coupling layer. The inset is the schematic of the OLEDs. Reproduced with permission.^[60] Copyright 2009, Elsevier. e) Schematic of a top-emission OLED device with textured morphology for light out-coupling enhancement. Reproduced with permission.^[62a] Copyright 2007, Elsevier.

microstructure has two functions. First, it enables the effective refractive index matching to the emission layer, which allows the energy to transfer across the thin (≈ 50 nm) metal layer. Second, the microstructure at the PR/air interface allows the SP modes to be out-coupled to light by Bragg scattering. As a result, the OCE was significantly enhanced.

Simply speaking, designing transparent or semitransparent top electrodes and recovering the SP mode loss with nano/micro-structures are the two most important methods for top-emission OLEDs. When it comes to the using of the active matrix for top-emission PeLEDs in the future, similar methods can be also utilized.

5.2.3. Light Out-Coupling for Polymer LEDs (PLEDs)

Specifically, PLEDs also have similar strategies to improve the OCE. McGehee and co-workers used Bragg gratings to couple out the waveguide modes.^[63] Li et al. used silver nanowires to improve the OCE of the white PLEDs.^[64] Kinner et al. used the ink jet-printed Ag/PEDOT:PSS electrode to improve the OCE of blue PLEDs.^[65] Based on material point-of-view, Lee et al. reported the OCE enhancement in liquid-crystalline fluorescent polymer (LCFP) films compared to the normal thermally annealed fluorescent films. The transverse electric (TE) waveguide mode can be suppressed due to the light scattering by liquid-crystalline

domains in the film.^[66] Moreover, Friend and co-workers fabricated self-organized, two-dimensional micrometer-scale photonic structures within the emission layer to improve the broadband waveguide mode out-coupling in polymer blend LEDs.^[67]

However, as organic LEDs include both small molecules (devices referred to as OLEDs)^[39,68] and conjugated-polymers (devices referred to as PLEDs),^[69] here we do not separate PLEDs from OLEDs in our further discussions.

5.3. Light Out-Coupling for Conventional Inorganic LEDs

The light out-coupling problems in inorganic conventional semiconductor LEDs have been studied for many years,^[70] and a lot of strategies can be adopted for PeLEDs. For instance, Zhong et al. used ZnO nanotips for GaN LED.^[71] Li et al. reported the top-down fabrication of InGaN/GaN nanorod LED arrays.^[72] Dae-Seob et al. textured the bottom side of the sapphire substrate to improve the OCE of the GaN flip-chip LEDs (FCLEDs).^[73] Intriguingly, Dolores-Calzadilla et al. talked about the nanoscale light sources using metal cavities for optical interconnects,^[74] and used grating coupler to collect the output power, with the OCE higher than 40%. And their nanopillar LED on silicon has the structure of n-InGaAs(100 nm)/n-InP(350 nm)/InGaAs(350 nm)/p-InP(600 nm)/p-InGaAsP(200 nm)/InP(250 nm)/SiO₂/benzo-cyclobutene (BCB)/SiO₂/Si. More

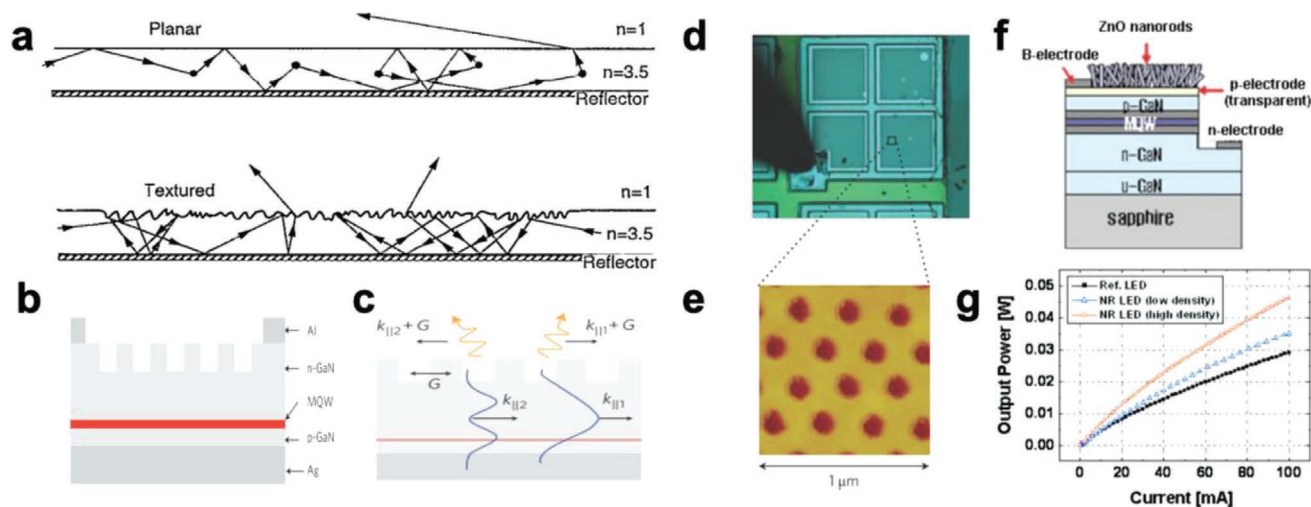


Figure 12. Light extraction for inorganic LEDs. a) 30% EQE surface textured AlGaAs-based LEDs. Reproduced with permission.^[19] Copyright 1993, American Institute of Physics. (b–e) Photonic crystal GaN LEDs with 73% light extraction. b) Diagram for the device. c) Diagram showing the conversion from guided modes (wavevector $k_{||}$) to leaky modes (leaky harmonic $k_{||} + G$). d) Optical photo of the device. e) The AFM image of the photonic crystal. Reproduced with permission.^[50d] Copyright 2009, Springer Nature. f,g) GaN LEDs with ZnO NR arrays. f) Diagram of the device structure. g) The output power of the devices with and without ZnO NR arrays. Reproduced with permission.^[83] Copyright 2009, American Institute of Physics.

significantly, Yablonoitch and co-workers discussed the light out-coupling in thin-slab InGaAs/InP LED.^[50b] Six-fold enhancement was achieved in PL, by using a 2D photonic crystal for highly efficient coherent external scattering of trapped light. Moreover, Delbeke et al. reviewed the resonant-cavity LEDs,^[75] together with some techniques based on gratings and photonic crystals. Leung et al. reviewed the light management in nanostructured LEDs.^[15k] Amano, Heremans, and co-workers summarized the issues on high-efficiency LEDs,^[76] and covered the out-coupling problem.

Figure 12 shows some of the classical light out-coupling strategies for inorganic LEDs. In 1993, Yablonoitch and co-workers discussed the significant gap between the IQE and the EQE and attributed the reason for the presence of the gap to the narrow light escape cone in high refractive index materials.^[19] By texturing the LEDs, they could improve the EQE from 9% to 30% for textured LED, compared to the planar counterpart. Figure 12a shows the photon trajectories in planar and textured structures respectively. The dots in the planar structure represent the self-absorption and re-emission processes which can be also called photon recycling.^[23,77] However, photon recycling only helps to increase the EQE when the material quality is high enough. In the textured structure,^[78] the surface scattering is very strong. Additionally, surface nanotexture can be formed by natural lithography.^[79] Moreover, the nanotexture is preferred to be at the half internal wavelength scale, which can give complete internal angular randomization of light rays in the emission layer.

Figure 12b–e are showing another typical method for light out-coupling improvement, which uses the photonic crystal structure to bring disturbance to the light trapping inside the LED device. Figure 12b is the GaN LED structure design reported by David and co-workers.^[50d] Figure 12c shows the key idea that photonic crystals can convert the laterally propagating guided modes^[80] to the leaky modes^[81] and therefore out-couple

the light more efficiently. As for the photonic crystal LEDs, Wiesmann et al. gave a comprehensive discussion in 2009 and more theoretical details can be found from their report.^[82] Figure 12d shows the optical photo of the GaN photonic crystal LED device and Figure 12e is the AFM image of the photonic crystal.

Figure 12f,g are showing another interesting idea to improve light out-coupling with ZnO NRs. Kim et al. reported enhanced light output efficiency by 57% when ZnO NRs were grown on the ITO electrode.^[83] Figure 12f is the device structure and Figure 12g shows the output power comparison between devices with and without ZnO NRs.

As for the PeLEDs, texturing the surface, using the photonic crystals, and using nanowires can all be explored for OCE enhancement.

5.4. Light Out-Coupling for QLEDs and MQWs LEDs

Quantum confinement can change the bandgap of the materials for luminance tunability and meanwhile increases the carriers/excitons confinement for more efficient radiative recombination in the active region.^[84] Colloidal QDs have tunable luminescence properties and can be deposited into a large area with the solution method.^[85] Sun et al. reported the bright infrared PbS QLEDs through inter-dot spacing control,^[85c] and mentioned that the choice of linker molecular can affect the OCE. Wang et al. used the nanoimprinting method to embed the grating patterns into the active layer of green CdSe@ZnS/ZnS QDs,^[86] and the gratings couple out the waveguide modes into the substrate. Moreover, they improved the EQE and luminance from 11.13% to 13.45%, and from 29010 to 44150 cd m^{-2} , respectively. In 2014, Sun and co-workers added a layer of ZnO nanopillars on the surface glass substrate to work as optical out-coupling medium,^[87] and they achieved the record high

CE (26.6 cd A^{-1}) and EQE (9.34%) for QLEDs at that time. The same group also reported the flexible top-emission QLEDs with a thin layer of Alq₃ (40 nm) as an optical out-coupling layer.^[88] Intriguingly, Wu and co-workers applied the dipole model to simulate the out-coupling and angular performance of QLEDs.^[89] In the dipole model, quantum dots are isotropic emitters in the multilayer system. Moreover, the multilayer structure can be simplified to a three-layer structure by the transfer matrix method.^[90] By combing the high refractive index glass substrate with macro-extractors, their simulations showed that the OCE can be doubled from $\approx 40\%$ to $\approx 80\%$. The same group also used FDTD simulations to analyze the light out-coupling in QLEDs and indicated that the random internal nanoscattering pattern can greatly enhance the OCE while maintaining the wide viewing angle for red light QLEDs.^[91]

MQWs have been successfully used for compound semiconductors for a long time.^[92] Moreover, MQWs LEDs can have strong carrier confinement and high carrier capture rate in the active region,^[93] and therefore have enhanced output power. Moreover, MQWs can also include light guiding layers, can have a resonance effect for lasing, and can have better material quality (e.g., remaining elastic strain in thin InGaN layer and increasing the crystal quality).^[94]

Bakin et al. used the metal-organic chemical vapor deposition (MOCVD) method to grow ZnO NRs for MQW InGaN/GaN LEDs.^[95] ZnO worked as both the n-type layer and the light out-coupling enhancement layer. Moreover, Dadgar et al. mentioned that the InGaN/GaN MQWs on Si substrate has three- to four-fold lesser light out-coupling than on the sapphire substrate.^[96] This is easy to understand because the index of sapphire is only 1.77 while the index of Si is ≈ 3.4 . Light from GaN ($n = 2.4$) can go to the lower index material more easily without concern of TIR at the interface. Furthermore, Kim et al. used the nanopatterned aluminum nitride to increase the OCE of the InGaN/GaN MQWs blue LED.^[97]

Coupling out more light in the lateral direction is another smart idea. In 2006, Shen et al. used sidewall texture and pillar waveguides (STPW) for InGaN/GaN MQWs LED to couple out the lateral guided modes.^[98] Moreover, Lee et al. reported the enhanced OCE of deep ultraviolet (DUV) Al_xGa_{1-x}N MQWs LEDs, and the strong TM-polarized light was coupled out from the sidewalls.^[99] They used the ray-tracing simulations to study the strong sidewall emission for efficient light out-coupling in the AlGaIn based DUV LED.

As for perovskite, according to Sargent and co-workers, the maneuver from bulk 3D perovskite (for solar cells) to reduced-dimensional structures is the central theme in perovskite light emission.^[1c] Note that the low dimensional perovskite together with compositional engineering has realized near-unity PLQY.^[1h,100] Moreover, MQWs structures of layered perovskite can have strong light-matter interactions, as discussed by Quan et al.^[1c] In 2016, Huang and co-workers reported the high EQE of 11.7% from self-organized MQWs perovskite LEDs thanks to the advantage of MQWs for efficient radiative decay.^[101] Particularly, colloidal nanometer-sized perovskite (especially Pb-free ones) nanocrystals (NCs) mixed with other polymers and small molecules with high PLQY can be used in displays as coatings.^[102] Although the perovskite QDs/NCs have been well studied,^[103] as far as we know, there is not much discussion

on the light out-coupling for perovskite QDs/MQWs LEDs, therefore the above-mentioned light out-coupling methods can be transferred to the perovskite QDs/MQWs LEDs for better performance.

5.5. Nanowires/Quantum Wires LEDs

Nanowire LEDs are a unique type of LED that can have intriguing capability to manipulate photons and electrons.^[104] Many interesting properties and applications can be studied and realized based on nanowire LEDs.^[105] In 2009, Yang and co-workers reviewed the nanowire photonics,^[106] and mentioned that nanowire LEDs can be categorized as crossed-nanowire junctions or forming longitudinal or co-axial heterojunctions.^[107] In 2006, Minot et al. reported the InP-InAsP nanowire LEDs by self-aligning the QDs,^[107d] and they mentioned that at the quantum optics region, nanowires can control the electron transport at the single electron level and light emission at the single-photon level.^[108] In 2009, Hersee et al. reported the vertically aligned GaN nanowire arrays with ≈ 300 nanowire p-n heterojunctions,^[109] and they indicated that the surface states did not dominate the device behavior of their nanowire LEDs. Intriguingly, Wang and co-workers also used the n-ZnO nanowire/GaN LED arrays for high-resolution imaging of the pressure distribution.^[110] Moreover, it is quite amazing that Mi and co-workers demonstrated the full-color (red, green, blue, and orange) single nanowire (InGaIn/GaN) pixels on a single chip, which can be used for projection displays.^[111] Another interesting study from the same group was that they found the Auger recombination plays a negligible role in the GaN nanowire LEDs which however suffer severely from the SRH recombination.^[112] In 2015, van Dam et al. reported the directional and polarized emission from nanowire LEDs.^[113] The far-field patterns and polarizations can be controlled by the nanowire diameters which determine the number and type of guided modes and leaky modes in the nanowires. Moreover, crossed nanowires were the first used to demonstrate the true nanoscale LEDs (nano LEDs).^[107a] Besides, nanowires can also be used as single-photon sources.^[114] Moreover, Kim et al. discussed that the light in nanowire LEDs can be efficiently coupled out from the large sidewall surfaces.^[115]

Intriguingly, perovskite nanowires can have near unity PLQY,^[8b,116] which can be even used for lasing.^[117] Additionally, perovskite micro-wires have also been reported for lasing, and a microdisk was used to couple out single-mode from the microwires.^[118] In 2019, we reported that the perovskite quantum wires showed much higher PLQY than perovskite nanowires due to both quantum confinement and the enhanced OCE.^[8b] Recently, we reported the vertical perovskite nanophotonic wire arrays LEDs with enhanced light out-coupling property. The OCE of perovskite nanowire LEDs was increased from $\approx 10\text{--}20\%$ to $\approx 40\text{--}50\%$, compared to the planar counterparts.^[119]

5.6. Light Out-Coupling Methods in Commercial LEDs

For commercial LEDs such as GaN LEDs, the index difference between GaN ($n = 2.4$) and air ($n = 1.0$) can be alleviated

by packaging, as a thin silicone ($n = 1.5$) layer can be added between the LED chip and air.^[120] Other common procedures can be adding an anti-reflection layer^[121] on the output side and reflection layer on the rear side.^[122] Particularly, the reflective layer can be diffraction Bragg reflector (DBR)^[123] or metallic layer with omnidirectional reflecting (ODR) coating.^[124] By dicing the chip into the inverted pyramid, which can be realized with the oblique focused laser beam, light out-coupling can also be improved.^[125] These kinds of LEDs are called truncated pyramidal LEDs (TP-LEDs). The light out-coupling enhancement for TP-LEDs can be simulated with the ray-tracing method.^[126]

FCLEDs were also proposed to utilize the large fraction of photons which emitted downward into substrates.^[127] FCLEDs usually use thick emission window layer, and the index difference between the sapphire substrate ($n = 1.7$) and the air is much smaller than GaN.^[128] There are also methods such as using photonic crystals,^[129] plasmonic nanostructures,^[130] micro-pillar arrays,^[131] and rough surfaces.^[132] The light out-coupling methods for commercial LEDs are quite generic and can be used for PeLEDs also.

5.7. Challenges for Adopting the Developed Strategies for PeLEDs

When it comes to the utilization of the developed strategies for PeLEDs, the compatibility needs to be considered case by case. We have introduced the refractive index properties in the previous discussions. The index is usually around 1.7 for organic emitter but larger than 2 for perovskites. And the index is even higher for inorganic semiconductors. Therefore, the optical design should be modified accordingly when applied to PeLEDs, as the out-coupling behavior is highly sensitive to the refractive index.

Meanwhile, adding nanostructures can also affect other perovskite properties such as the charge carrier/exciton recombinations.^[133] Although this review is focused on the optical design of PeLEDs, we also want to draw the attention to whether adding nanostructures can affect material deposition qualities (uniformity, crystallinities, defects, etc.),^[16b] balanced charge carrier injections,^[35] etc. Applying nanostructures outside perovskite emissive layer can have less effect (either positive or negative) on altering material properties, but directly applying nanostructures to perovskite itself is sometimes necessary, e.g., to introduce the quantum confinement effect,^[8b] or the internal light scatterings.^[2a]

Although there are some reports on the vapor fabrication of PeLEDs,^[134] most of the PeLEDs are still fabricated with solution methods. As for OLEDs, both dry methods (e.g., vacuum evaporation with fine metal masks) and wet methods (e.g., ink-jet printing, nozzle printing, relief printing, etc.) have been well developed.^[135] Therefore, the fabrication compatibility (wet or dry processes; with or without post-annealing, etc.) need to be carefully considered when applying the strategies for evaporated OLEDs to the solution-fabricated PeLEDs. Moreover, whether solution method can produce uniformly deposited films is another concern when fabricating devices on nanostructures. This is one of the reasons why developing vapor fabrication process for PeLEDs is important in terms of scalability

and uniformity. Besides, solvents for perovskites and other materials can also be different. For example, the common solvents for perovskite materials are dimethylformamide (DMF) and dimethyl sulfoxide (DMSO). For perovskite NCs/QDs, the solvents/dispersion solutions can be γ -butyrolactone,^[136] toluene,^[137] *n*-octylamine (OLAm)/DMF/oleic acids (OA),^[138] hexane,^[139] etc., while the solvents for polymer emitters can be common organic solvents (toluene, xylene, tetrahydrofuran, chloroform, chlorobenzene, cyclohexanone, etc.)^[140] The solvent difference should also be considered during the fabrication processes for nanostructures or devices.

5.8. The Simulation Methods for Light Out-Coupling Study in PeLEDs

For OLED, researchers treated the exciton as radiating dipole emitters in the forward calculation out-coupling model.^[141] Furthermore, Lee et al. used the Monte Carlo modeling to analyze the OCE for PLEDs.^[142] In order to experimentally define the OCE, van Mensfoort et al. proposed solving the inverse out-coupling problem by measuring the light emission profile in OLEDs.^[141a] And knowing the light emission profile with high accuracy can be potentially used to calculate the OCE and thereafter deduce the IQE from EQE.

To study the light out-coupling in PeLED devices, a few groups have reported the simulation methods to calculate the light OCEs.^[2a,9,16b,18,143] For instance, Qin et al. used SETFOS 4.5 software to calculate light out-coupling, and modeled the excitons with isotropic radiative dipoles.^[143] They also weighed the power radiated from dipole by the PL spectrum from the emission layer. Moreover, they can also calculate the dissipated power with different wavelengths.

Huang and co-workers used the FDTD method and studied the light out-coupling in the self-formed micro-structured infrared PeLEDs (simulation wavelength 800 nm).^[2a] The refractive indexes were measured with an ellipsometer (KLA-Tencor, P7), and the imaginary part of the perovskite index was ignored. Nine uniformly distributed sources were used, and the average result was taken. Because the micro-structures have the light scattering effect, the overall light OCE was improved to about 30% (this OCE was verified by the 30% EQE when cooling down the temperature to 6 K, in which case the IQE can be assumed as 100%). As a comparison, the planar structure only has a light OCE of about 21.8%.

Moreover, Tang and co-workers also used the FDTD method together with custom-made MATLAB codes to study the cross-sectional electrical field patterns. The light energy distribution can be resolved to help understand the light out-coupling process in PeLED devices (simulation wavelength 514 nm).^[18d] Emission dipoles with horizontal directions (parallel to the substrate) at three locations were used. The photon number at 514 nm was fixed for the Gaussian oscillating dipole pulse to monitor the light intensity and to compare the relative OCE.

In 2018, Gao and co-workers reported a theoretical study of the light energy distributions in the PeLED devices and revealed that the maximum EQEs for 3D perovskite and quasi-2D perovskite LEDs are about 25% and 20%, respectively.^[35] The simulation methods that Gao and co-workers used were the

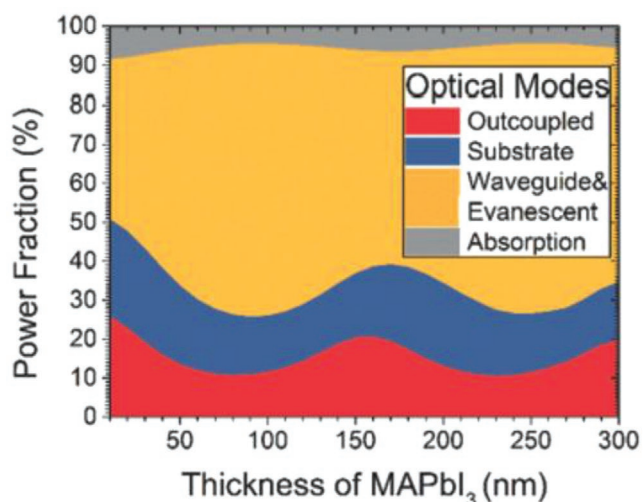


Figure 13. Power fraction of different modes in MAPbI₃ PeLEDs. Reproduced with permission.^[35] Copyright 2018, Wiley-VCH.

Transfer Matrix approach and the FDTD method. The former was developed for modeling the multilayer OLEDs. The EM simulation model treats the radiative decay of excitonic species as an assembly of classical electrical dipole antennas. Moreover, they made the following assumptions in the simulation. First, the dipole orientation is isotropic. Moreover, they mentioned that horizontal dipole had a fraction of $2/3$ in the isotropic case. Second, they assumed the properties of all materials were isotropic. Third, the emission layer did not absorb light in the emission region. Fourth, they used a discrete emitter position. Particularly, the emitters were located at the emission layer/injection layer interface. Last, they assumed the device worked at low excitation levels and ignored the Auger recombination. It is worth noting that the boundary condition perpendicular to the interfaces was Bloch, which is important when the light is not normal incidence/emission in the periodical structures. Moreover, the refractive indexes of MAPbI₃ and NFPI₇ are about 2.6 and 2.0, respectively. They also studied the perovskite index range from 1.75 to 3.00 to get a comprehensive result. **Figure 13** shows the power distribution of different modes in the PeLEDs. The maximum OCE of 25.7% can be achieved. A more detailed optical mode analysis was done and perfectly explained in their work.^[35] Furthermore, to simply ascertain the light OCE in OLEDs and PeLEDs, the following formula can be used^[144]

$$\text{OCE} \approx \frac{1}{2n^2} \quad (6)$$

where the n is the refractive index of the emission layer. Noting that the $0.5 n^{-2}$ relation is for the estimation of surface OCE with the isotropic dipoles (not subject to the optical interference with the metal reflector). When it comes to the surface OCE with the inplane dipoles (not subject to the optical interference with the metal reflector), $0.75 n^{-2}$ should be used. More details should be referred to the discussion given by Friend and co-workers.^[144]

Rand and co-workers also had a few reports discussing the light out-coupling for PeLEDs.^[18a,b] The simulation methods

used by them were a classical oscillating dipole model^[18b,145] and the FDTD method.^[18a] For the simulation based on the oscillating dipole model, the Rand group made the following assumptions. First, the emission zone was confined to an infinitely thin zone. (This can simplify the light source to a planar one.) Second, the IQE was unity. Third, the emission pattern was isotropic. Fourth, there was not electrical loss. For the FDTD simulation, the boundary conditions on the $\pm x$ and $\pm y$ directions were perfectly matching layer (PML). The dipole sources oriented along x -, y -, and z -directions were located in the middle of the emission layer. The far field was calculated over a 1 m radius hemisphere surface.

Last but not least, our group has also reported the study on the light out-coupling in PeLED devices on nanophotonic substrates previously.^[10b] We performed a systematic study on the geometry effect with FDTD method and found that the nanostructure geometry must be optimized otherwise light OCE can be even decreased. Only when the nanostructure is properly designed, a huge enhancement in light OCE can be achieved (e.g., from 10% to 73% with a sevenfold enhancement). In our study, we used the dipole sources with different locations and polarization directions and took the average light OCE as the final result. Moreover, the light OCE can be calculated from the light power collected by the monitor in the air over the light power collected by the transmission box surrounding the dipole light source. The periodic boundary conditions can be used in the lateral direction when the nanostructures are in periodic arrays. Cross-sectional E^2 intensities were also recorded both in the frequency domain and time domain. The frequency-domain result shows the electrical field and power distribution; while the time domain result records the whole light propagation processes. Moreover, when the multiple wavelengths result is required, the simulation has to be conducted wavelength by wavelength to avoid the discrepancy in the material index fitting data with the input material n and k values. With the above-discussed method, we also studied the light out-coupling in the MAPbI₃ perovskite quantum wires.^[8b] When the diameter of the wires decreases to a few nanometers, the quantum confinement will come into play. And it increases the PLQY from 0.81% to 45.1%. More significantly, the light OCE of the 5.7 nm diameter quantum wire can achieve a high value of 90.6%. Lately, we had another work discussing the light out-coupling behaviors inside perovskite nanowires.^[119] With the FDTD simulations, we found that the nanophotonic effects can be very complex in the nanowire arrays. Optical resonances such as Mie resonances,^[146] surface lattice resonances,^[147] and Fabry–Perot resonances^[148] can exist in the nanowires and together they determine the light behaviors in the nanowires. In order to get a clearer picture of the detailed mechanisms, more work needs to be done in the future.

6. Conclusion

In this review, we first introduced an account of the rapid development of PeLEDs. Then we demonstrated that the perovskite materials have a high refractive index and therefore the OCE is the key to further improve the EQE of PeLEDs. Moreover, as PeLEDs always have high material quality and high IQE,

photon recycling can make the out-coupling a multiple re-absorption and re-emission process. After that, we reviewed the out-coupling methods that have been used for the PeLEDs, although less explored. Then we thoroughly went through the light out-coupling studies for OLEDs, conventional semiconductor LEDs, QLEDs, MQWs LEDs, nanowire LEDs, and commercial LEDs. By reviewing those reports, we can summarize a set of general guidelines for the out-coupling design. First, introducing structures comparable to wavelength scale (e.g., photonic crystals, isolated NCs, buckled structures) into active material or tuning the thickness of the active layer can couple out the waveguide modes. Second, adding structures (e.g., hemisphere injection material, NHAs, metal NPs, low-index grids, gratings, photonic crystals) between the active layer and transparent electrodes can couple the waveguide modes to substrate modes. Third, adding structures (e.g., nanowires or nanorods, photonic crystals) to the glass can couple the substrate mode to light emission. As for top-emission LEDs, the out-coupling strategies also include designing the translucent top electrodes for better transparency and adding structures at the electrode interface to out-couple SP modes to air. Moreover, we also summarized the simulation methods for studying the out-coupling for PeLEDs and discussed a few examples of simulation condition settings. Overall, in this review, we provide clear and systematic guidelines for light out-coupling enhancement with nanophotonic engineering, which pave the way for high-performance PeLEDs fabrication in the future.

Acknowledgements

This work was supported by National Natural Science Foundation of China (Project No. 51672231), Shen Zhen Science and Technology Innovation Commission (Project No. JCYJ20170818114107730), HKUST Fund of Nanhai (Grant No. FSNH-18FYTR101), and Hong Kong Research Grant Council (General Research Fund Project No. 16237816, 16309018). The authors also acknowledge the support from the Center for 1D/2D Quantum Materials and the State Key Laboratory of Advanced Displays and Optoelectronics Technologies at HKUST.

Conflict of Interest

The authors declare no conflict of interest.

Keywords

light-emitting diodes, light out-coupling, nanophotonic engineering, perovskites, simulations

Received: March 20, 2020
Revised: April 12, 2020
Published online:

- [1] a) B. R. Sutherland, E. H. Sargent, *Nat. Photonics* **2016**, *10*, 295; b) S. D. Stranks, R. L. Hoyer, D. Di, R. H. Friend, F. Deschler, *Adv. Mater.* **2018**, *31*, 1803336; c) L. N. Quan, B. P. Rand, R. H. Friend, S. G. Mhaisalkar, T.-W. Lee, E. H. Sargent, *Chem. Rev.* **2019**, *119*, 7444; d) X. Zhao, J. D. A. Ng, R. H. Friend, Z.-K. Tan, *ACS*

- Photonics* **2018**, *5*, 3866; e) S. D. Stranks, H. J. Snaith, *Nat. Nanotechnol.* **2015**, *10*, 391; f) M.-H. Park, J. S. Kim, J.-M. Heo, S. Ahn, S.-H. Jeong, T.-W. Lee, *ACS Energy Lett.* **2019**, *4*, 1134; g) Z. Wei, J. Xing, *J. Phys. Chem. Lett.* **2019**, *10*, 3035; h) M. Yuan, L. N. Quan, R. Comin, G. Walters, R. Sabatini, O. Voznyy, S. Hoogland, Y. Zhao, E. M. Beaugregard, P. Kanjanaboos, *Nat. Nanotechnol.* **2016**, *11*, 872; i) Y.-H. Kim, H. Cho, T.-W. Lee, *Proc. Natl. Acad. Sci. USA* **2016**, *113*, 11694; j) Q. Shan, J. Song, Y. Zou, J. Li, L. Xu, J. Xue, Y. Dong, B. Han, J. Chen, H. Zeng, *Small* **2017**, *13*, 1701770; k) P. Fan, D. Gu, G.-X. Liang, J.-T. Luo, J.-L. Chen, Z.-H. Zheng, D.-P. Zhang, *Sci. Rep.* **2016**, *6*, 29910; l) G.-X. Liang, P. Fan, J.-T. Luo, D. Gu, Z.-H. Zheng, *Prog. Photovoltaics* **2015**, *23*, 1901.
- [2] a) Y. Cao, N. Wang, H. Tian, J. Guo, Y. Wei, H. Chen, Y. Miao, W. Zou, K. Pan, Y. He, H. Cao, Y. Ke, M. Xu, Y. Wang, M. Yang, K. Du, Z. Fu, D. Kong, D. Dai, Y. Jin, G. Li, H. Li, Q. Peng, J. Wang, W. Huang, *Nature* **2018**, *562*, 249; b) T. Chiba, Y. Hayashi, H. Ebe, K. Hoshi, J. Sato, S. Sato, Y.-J. Pu, S. Ohisa, J. Kido, *Nat. Photonics* **2018**, *12*, 681; c) K. Lin, J. Xing, L. N. Quan, F. P. G. de Arquer, X. Gong, J. Lu, L. Xie, W. Zhao, D. Zhang, C. Yan, W. Li, X. Liu, Y. Lu, J. Kirman, E. H. Sargent, Q. Xiong, Z. Wei, *Nature* **2018**, *562*, 245.
- [3] a) Y. Liu, J. Cui, K. Du, H. Tian, Z. He, Q. Zhou, Z. Yang, Y. Deng, D. Chen, X. Zuo, Y. Ren, L. Wang, H. Zhu, B. Zhao, D. Di, J. Wang, R. H. Friend, Y. Jin, *Nat. Photonics* **2019**, *13*, 760; b) C.-H. A. Li, Z. Zhou, P. Vashishtha, J. E. Halpert, *Chem. Mater.* **2019**, *31*, 6003; c) Q. Wang, X. Wang, Z. Yang, N. Zhou, Y. Deng, J. Zhao, X. Xiao, P. Rudd, A. Moran, Y. Yan, J. Huang, *Nat. Commun.* **2019**, *10*, 5633.
- [4] S. D. Stranks, *ACS Energy Lett.* **2017**, *2*, 1515.
- [5] a) P. Vashishtha, J. E. Halpert, *Chem. Mater.* **2017**, *29*, 5965; b) M. Chen, X. Shan, T. Geske, J. Li, Z. Yu, *ACS Nano* **2017**, *11*, 6312; c) P. Calado, A. M. Telford, D. Bryant, X. Li, J. Nelson, B. C. O'Regan, P. R. Barnes, *Nat. Commun.* **2016**, *7*, 13831; d) Z. Xiao, R. A. Kerner, L. Zhao, N. L. Tran, K. M. Lee, T.-W. Koh, G. D. Scholes, B. P. Rand, *Nat. Photonics* **2017**, *11*, 108; e) L. Zhao, J. Gao, Y. L. Lin, Y. W. Yeh, K. M. Lee, N. Yao, Y. L. Loo, B. P. Rand, *Adv. Mater.* **2017**, *29*, 1605317; f) Y.-H. Kim, C. Wolf, H. Kim, T.-W. Lee, *Nano Energy* **2018**, *52*, 329.
- [6] J. M. Richter, M. Abdi-Jalebi, A. Sadhanala, M. Tabachnyk, J. P. Rivett, L. M. Pazos-Outón, K. C. Gödel, M. Price, F. Deschler, R. H. Friend, *Nat. Commun.* **2016**, *7*, 13941.
- [7] C. Wehrenfennig, M. Liu, H. J. Snaith, M. B. Johnston, L. M. Herz, *J. Phys. Chem. Lett.* **2014**, *5*, 1300.
- [8] a) I. L. Braly, D. W. deQuilettes, L. M. Pazos-Outón, S. Burke, M. E. Ziffer, D. S. Ginger, H. W. Hillhouse, *Nat. Photonics* **2018**, *12*, 355; b) D. Zhang, L. Gu, Q. Zhang, Y. Lin, D.-H. Lien, M. Kam, S. Poddar, E. C. Garnett, A. Javey, Z. Fan, *Nano Lett.* **2019**, *19*, 2850.
- [9] Z. Shi, S. Li, Y. Li, H. Ji, X. Li, D. Wu, T. Xu, Y. Chen, Y. Tian, Y. Zhang, *ACS Nano* **2018**, *12*, 1462.
- [10] a) M. S. Alias, I. Dursun, M. I. Saidaminov, E. M. Diallo, P. Mishra, T. K. Ng, O. M. Bakr, B. S. Ooi, *Opt. Express* **2016**, *24*, 16586; b) Q. Zhang, M. M. Tavakoli, L. Gu, D. Zhang, L. Tang, Y. Gao, J. Guo, Y. Lin, S.-F. Leung, S. Poddar, Y. Fu, Z. Fan, *Nat. Commun.* **2019**, *10*, 727.
- [11] a) A. Miyata, A. Mitioglu, P. Plochocka, O. Portugall, J. T.-W. Wang, S. D. Stranks, H. J. Snaith, R. J. Nicholas, *Nat. Phys.* **2015**, *11*, 582; b) Q. Lin, A. Armin, R. C. R. Nagiri, P. L. Burn, P. Meredith, *Nat. Photonics* **2015**, *9*, 106.
- [12] a) N. M. Ravindra, P. Ganapathy, J. Choi, *Infrared Phys. Technol.* **2007**, *50*, 21; b) P. Hervé, L. K. J. Vandamme, *Infrared Phys. Technol.* **1994**, *35*, 609.
- [13] T. S. Moss, *Proc. Phys. Soc., Sect. A* **1951**, *64*, 590.
- [14] L. H. Smith, W. L. Barnes, *Org. Electron.* **2006**, *7*, 490.
- [15] a) H. Yang, M. Chen, S. Wang, presented at *16th International Conference on Electronic Packaging Technology (ICEPT)*, **2015**; b) M.-H. Shin, H.-G. Hong, Y.-J. Kim, presented at *17th Microoptics*

- Conference (MOC), **2011**; c) X. Xu, H. Li, Y. Zhuo, D. Xiong, M. Chen, *J. Am. Ceram. Soc.* **2019**, *102*, 1677; d) S. Yang, J. S. Kim, J. Jin, S. Y. Kwak, B. S. Bae, *J. Appl. Polym. Sci.* **2011**, *122*, 2478; e) M. Ma, F. W. Mont, X. Yan, J. Cho, E. F. Schubert, G. B. Kim, C. Sone, *Opt. Express* **2011**, *19*, A1135; f) C.-M. Hsu, C. Battaglia, C. Pahud, Z. Ruan, F.-J. Haug, S. Fan, C. Ballif, Y. Cui, *Adv. Energy Mater.* **2012**, *2*, 628; g) J. Zhu, Z. Yu, G. F. Burkhard, C.-M. Hsu, S. T. Connor, Y. Xu, Q. Wang, M. McGehee, S. Fan, Y. Cui, *Nano Lett.* **2009**, *9*, 279; h) S. Jeong, E. C. Garnett, S. Wang, Z. Yu, S. Fan, M. L. Brongersma, M. D. McGehee, Y. Cui, *Nano Lett.* **2012**, *12*, 2971; i) Y. Qiu, S.-F. Leung, Q. Zhang, B. Hua, Q. Lin, Z. Wei, K.-H. Tsui, Y. Zhang, S. Yang, Z. Fan, *Nano Lett.* **2014**, *14*, 2123; j) M. M. Tavakoli, K.-H. Tsui, Q. Zhang, J. He, Y. Yao, D. Li, Z. Fan, *ACS Nano* **2015**, *9*, 10287; k) S.-F. Leung, Q. Zhang, F. Xiu, D. Yu, J. C. Ho, D. Li, Z. Fan, *J. Phys. Chem. Lett.* **2014**, *5*, 1479; l) Y. Qiu, S.-F. Leung, Q. Zhang, C. Mu, B. Hua, H. Yan, S. Yang, Z. Fan, *Sci. Bull.* **2015**, *60*, 109; m) L. Tang, K.-H. Tsui, S.-F. Leung, Q. Zhang, M. Kam, H.-P. Wang, J.-H. He, Z. Fan, *J. Semicond.* **2019**, *40*, 042601.
- [16] a) S.-i. Inoue, N. Tamari, M. Taniguchi, *Appl. Phys. Lett.* **2017**, *110*, 141106; b) Q. Zhang, M. M. Tavakoli, L. Gu, D. Zhang, L. Tang, Y. Gao, J. Guo, Y. Lin, S.-F. Leung, S. Poddar, *Nat. Commun.* **2019**, *10*, 727; c) K. Okamoto, Y. Kawakami, *IEEE J. Sel. Top. Quantum Electron.* **2009**, *15*, 1199; d) G. Lozano, D. J. Louwers, S. R. Rodríguez, S. Murai, O. T. Jansen, M. A. Verschuuren, J. G. Rivas, *Light: Sci. Appl.* **2013**, *2*, e66; e) C. Huh, K.-S. Lee, E.-J. Kang, S.-J. Park, *J. Appl. Phys.* **2003**, *93*, 9383.
- [17] a) Z. Fan, H. Razavi, J.-w. Do, A. Moriwaki, O. Ergen, Y.-L. Chueh, P. W. Leu, J. C. Ho, T. Takahashi, L. A. Reichertz, S. Neale, K. Yu, M. Wu, J. W. Ager, A. Javey, *Nat. Mater.* **2009**, *8*, 648; b) X. Liu, L. Gu, Q. Zhang, J. Wu, Y. Long, Z. Fan, *Nat. Commun.* **2014**, *5*, 4007; c) J. Li, Y. Qiu, Z. Wei, Q. Lin, Q. Zhang, K. Yan, H. Chen, S. Xiao, Z. Fan, S. Yang, *Energy Environ. Sci.* **2014**, *7*, 3651; d) J. Lee, Q. Zhang, S. Park, A. Choe, Z. Fan, H. Ko, *ACS Appl. Mater. Interfaces* **2016**, *8*, 634; e) L. Wu, Z. Yang, M. Zhao, Y. Yu, S. Li, Q. Zhang, X. Yuan, *Opt. Express* **2011**, *19*, 17539; f) Y. Zhu, Q. Zhang, M. Kam, S. Poddar, L. Gu, S. Liang, P. Qi, F. Miao, Z. Fan, *InfoMat* **2019**, <https://doi.org/10.1002/inf2.12070>.
- [18] a) S. Jeon, L. Zhao, Y. J. Jung, J. W. Kim, S. Y. Kim, H. Kang, J. H. Jeong, B. P. Rand, J. H. Lee, *Small* **2019**, *15*, 1900135; b) L. Zhao, K. M. Lee, K. Roh, S. U. Z. Khan, B. P. Rand, *Adv. Mater.* **2019**, *31*, 1805836; c) S.-S. Meng, Y.-Q. Li, J.-X. Tang, *Org. Electron.* **2018**, *61*, 351; d) Y. Shen, L. P. Cheng, Y. Q. Li, W. Li, J. D. Chen, S. T. Lee, J. X. Tang, *Adv. Mater.* **2019**, *31*, 1901517.
- [19] I. Schnitzer, E. Yablonovitch, C. Caneau, T. Gmitter, A. Scherer, *Appl. Phys. Lett.* **1993**, *63*, 2174.
- [20] J.-S. Kim, P. K. Ho, N. C. Greenham, R. H. Friend, *J. Appl. Phys.* **2000**, *88*, 1073.
- [21] T. Fujii, Y. Gao, R. Sharma, E. Hu, S. DenBaars, S. Nakamura, *Appl. Phys. Lett.* **2004**, *84*, 855.
- [22] I. Dursun, Y. Zheng, T. Guo, M. De Bastiani, B. Turedi, L. Sinatra, M. A. Haque, B. Sun, A. A. Zhumekenov, M. I. Saidaminov, *ACS Energy Lett.* **2018**, *3*, 1492.
- [23] L. M. Pazos-Outón, M. Szumilo, R. Lamboll, J. M. Richter, M. Crespo-Quesada, M. Abdi-Jalebi, H. J. Beeson, M. Vručinić, M. Alsari, H. J. Snaith, B. Ehrler, R. H. Friend, F. Deschler, *Science* **2016**, *351*, 1430.
- [24] E. F. Schubert, T. Gessmann, J. K. Kim, *Kirk-Othmer Encycl. Chem. Technol.* **2000**.
- [25] P. Löper, M. Stuckelberger, B. Niesen, J. Werner, M. Filipič, S.-J. Moon, J.-H. Yum, M. Topič, S. De Wolf, C. Ballif, *J. Phys. Chem. Lett.* **2015**, *6*, 66.
- [26] M. A. Green, Y. Jiang, A. M. Soufiani, A. Ho-Baillie, *J. Phys. Chem. Lett.* **2015**, *6*, 4774.
- [27] E. D. Palik, *Handbook of Optical Constants of Solids*, Academic Press, MA **1998**.
- [28] S. Wemple, M. DiDomenico Jr., *Phys. Rev. B* **1971**, *3*, 1338.
- [29] Z. Xie, S. Liu, L. Qin, S. Pang, W. Wang, Y. Yan, L. Yao, Z. Chen, S. Wang, H. Du, *Opt. Mater. Express* **2015**, *5*, 1998.
- [30] a) I. Suárez, E. J. Juárez-Pérez, J. Bisquert, I. Mora-Seró, J. P. Martínez-Pastor, *Adv. Mater.* **2015**, *27*, 6157; b) Y. J. Li, Y. Lv, C.-L. Zou, W. Zhang, J. Yao, Y. S. Zhao, *J. Am. Chem. Soc.* **2016**, *138*, 2122; c) Z. Wang, J. Liu, Z.-Q. Xu, Y. Xue, L. Jiang, J. Song, F. Huang, Y. Wang, Y. L. Zhong, Y. Zhang, Y.-B. Cheng, Q. Bao, *Nanoscale* **2016**, *8*, 6258; d) G. L. Whitworth, J. R. Harwell, D. N. Miller, G. J. Hedley, W. Zhang, H. J. Snaith, G. A. Turnbull, I. D. W. Samuel, *Opt. Express* **2016**, *24*, 23677; e) I. Dursun, Y. Zheng, T. Guo, M. De Bastiani, B. Turedi, L. Sinatra, M. A. Haque, B. Sun, A. A. Zhumekenov, M. I. Saidaminov, F. P. García de Arquer, E. H. Sargent, T. Wu, Y. N. Gartstein, O. M. Bakr, O. F. Mohammed, A. V. Malko, *ACS Energy Lett.* **2018**, *3*, 1492; f) Y. Zhang, J. Liu, Z. Wang, Y. Xue, Q. Ou, L. Polavarapu, J. Zheng, X. Qi, Q. Bao, *Chem. Commun.* **2016**, *52*, 13637.
- [31] a) X. Wu, L. Z. Tan, X. Shen, T. Hu, K. Miyata, M. T. Trinh, R. Li, R. Coffee, S. Liu, D. A. Egger, *Sci. Adv.* **2017**, *3*, e1602388; b) G. Y. Kim, A. Senocrate, T.-Y. Yang, G. Gregori, M. Grätzel, J. Maier, *Nat. Mater.* **2018**, *17*, 445; c) Y. Zhou, L. You, S. Wang, Z. Ku, H. Fan, D. Schmidt, A. Rusydi, L. Chang, L. Wang, P. Ren, *Nat. Commun.* **2016**, *7*, 11913.
- [32] a) L. Gao, L. N. Quan, F. P. García de Arquer, Y. Zhao, R. Munir, A. Proppe, R. Quintero-Bermudez, C. Zou, Z. Yang, M. I. Saidaminov, O. Voznyy, S. Kinger, Z. Lu, S. O. Kelley, A. Amassian, J. Tang, E. H. Sargent, *Nat. Photonics* **2020**, *14*, 227; b) H. Chen, J. Lin, J. Kang, Q. Kong, D. Lu, J. Kang, M. Lai, L. N. Quan, Z. Lin, J. Jin, L.-w. Wang, M. F. Toney, P. Yang, *Sci. Adv.* **2020**, *6*, eaay4045; c) Z. Li, Z. Chen, Y. Yang, Q. Xue, H.-L. Yip, Y. Cao, *Nat. Commun.* **2019**, *10*, 1027; d) T. Wu, J. Li, Y. Zou, H. Xu, K. Wen, S. Wan, S. Bai, T. Song, J. A. McLeod, S. Duhm, F. Gao, B. Sun, *Angew. Chem., Int. Ed.* **2020**, *59*, 4099; e) Y. Shang, Y. Liao, Q. Wei, Z. Wang, B. Xiang, Y. Ke, W. Liu, Z. Ning, *Sci. Adv.* **2019**, *5*, eaaw8072; f) W. Deng, X. Jin, Y. Lv, X. Zhang, X. Zhang, J. Jie, *Adv. Funct. Mater.* **2019**, *29*, 1903861.
- [33] M. Anaya, B. P. Rand, R. J. Holmes, D. Credgington, H. J. Bolink, R. H. Friend, J. Wang, N. C. Greenham, S. D. Stranks, *Nat. Photonics* **2019**, *13*, 818.
- [34] a) N. C. Greenham, R. H. Friend, D. D. Bradley, *Adv. Mater.* **1994**, *6*, 491; b) S. R. Forrest, D. D. Bradley, M. E. Thompson, *Adv. Mater.* **2003**, *15*, 1043; c) H. J. Snaith, *Nat. Photonics* **2012**, *6*, 337.
- [35] X. B. Shi, Y. Liu, Z. Yuan, X. K. Liu, Y. Miao, J. Wang, S. Lenk, S. Reineke, F. Gao, *Adv. Opt. Mater.* **2018**, *6*, 1800667.
- [36] J. B. Schneider, **2010**, 181.
- [37] B. Zhao, S. Bai, V. Kim, R. Lamboll, R. Shivanna, F. Auras, J. M. Richter, L. Yang, L. Dai, M. Alsari, X.-J. She, L. Liang, J. Zhang, S. Lilliu, P. Gao, H. J. Snaith, J. Wang, N. C. Greenham, R. H. Friend, D. Di, *Nat. Photonics* **2018**, *12*, 783.
- [38] W. Helfrich, W. Schneider, *Phys. Rev. Lett.* **1965**, *14*, 229.
- [39] C. W. Tang, S. A. VanSlyke, *Appl. Phys. Lett.* **1987**, *51*, 913.
- [40] Y. Karzazi, *J. Mater. Environ. Sci.* **2014**, *5*, 1.
- [41] a) C. Adachi, M. A. Baldo, M. E. Thompson, S. R. Forrest, *J. Appl. Phys.* **2001**, *90*, 5048; b) M. A. Baldo, D. O'Brien, Y. You, A. Shoustikov, S. Sibley, M. Thompson, S. R. Forrest, *Nature* **1998**, *395*, 151.
- [42] a) L. H. Smith, J. A. Wasey, I. D. Samuel, W. L. Barnes, *Adv. Funct. Mater.* **2005**, *15*, 1839; b) P. A. Hobson, S. Wedge, J. A. Wasey, I. Sage, W. L. Barnes, *Adv. Mater.* **2002**, *14*, 1393; c) A. Chutinan, K. Ishihara, T. Asano, M. Fujita, S. Noda, *Org. Electron.* **2005**, *6*, 3.
- [43] V. Bulović, V. Khalfin, G. Gu, P. Burrows, D. Garbuzov, S. Forrest, *Phys. Rev. B* **1998**, *58*, 3730.
- [44] Y. Gu, D.-D. Zhang, Q.-D. Ou, Y.-H. Deng, J.-J. Zhu, L. Cheng, Z. Liu, S.-T. Lee, Y.-Q. Li, J.-X. Tang, *J. Mater. Chem. C* **2013**, *1*, 4319.
- [45] J.-L. Wu, F.-C. Chen, Y.-S. Hsiao, F.-C. Chien, P. Chen, C.-H. Kuo, M. H. Huang, C.-S. Hsu, *ACS Nano* **2011**, *5*, 959.

- [46] Y. Sun, S. R. Forrest, *Nat. Photonics* **2008**, 2, 483.
- [47] T. Tsutsui, M. Yahiro, H. Yokogawa, K. Kawano, M. Yokoyama, *Adv. Mater.* **2001**, 13, 1149.
- [48] a) M. Slootsky, S. R. Forrest, *Opt. Lett.* **2010**, 35, 1052; b) W. H. Koo, S. M. Jeong, F. Araoka, K. Ishikawa, S. Nishimura, T. Toyooka, H. Takezoe, *Nat. Photonics* **2010**, 4, 222.
- [49] Y. Qu, M. Slootsky, S. R. Forrest, *Nat. Photonics* **2015**, 9, 758.
- [50] a) J. D. Joannopoulos, P. R. Villeneuve, S. Fan, *Nature* **1997**, 386, 143; b) M. Boroditsky, T. Krauss, R. Coccioli, R. Vrijen, R. Bhat, E. Yablonovitch, *Appl. Phys. Lett.* **1999**, 75, 1036; c) H. Ryu, Y.-H. Lee, R. Sellin, D. Bimberg, *Appl. Phys. Lett.* **2001**, 79, 3573; d) J. J. Wierer Jr., A. David, M. M. Megens, *Nat. Photonics* **2009**, 3, 163; e) Y. R. Do, Y. C. Kim, Y. W. Song, C. O. Cho, H. Jeon, Y. J. Lee, S. H. Kim, Y. H. Lee, *Adv. Mater.* **2003**, 15, 1214.
- [51] a) D. Fyfe, *Nat. Photonics* **2009**, 3, 453; b) S. Hofmann, M. Thomschke, B. Lüssem, K. Leo, *Opt. Express* **2011**, 19, A1250.
- [52] J. Meyer, P. Görrn, S. Hamwi, H.-H. Johannes, T. Riedl, W. Kowalsky, *Appl. Phys. Lett.* **2008**, 93, 073308.
- [53] C. Lee, R. Pode, D. Moon, J. Han, *Thin Solid Films* **2004**, 467, 201.
- [54] S. Han, X. Feng, Z. Lu, D. Johnson, R. Wood, *Appl. Phys. Lett.* **2003**, 82, 2715.
- [55] S. D. Yambem, M. Ullah, K. Tandy, P. L. Burn, E. B. Namdas, *Laser Photonics Rev.* **2014**, 8, 165.
- [56] a) C.-J. Lee, Y.-I. Park, J.-H. Kwon, J.-W. Park, *Bull. Korean Chem. Soc.* **2005**, 26, 1344; b) S. Chen, X. Li, W. Huang, *Org. Electron.* **2008**, 9, 1112; c) S. M. Jeong, Y. Takanishi, K. Ishikawa, S. Nishimura, G. Suzuki, H. Takezoe, *Opt. Commun.* **2007**, 273, 167.
- [57] a) H. Antoniadis, F. Doerfel, *U.S. Patent 7,489,074[P]*, **2009**; b) V.-E. Choong, F. So, *U.S. Patent Application 10/951,514[P]*, **2006**; c) N. Tessler, S. Burns, H. Becker, R. Friend, *Appl. Phys. Lett.* **1997**, 70, 556; d) X.-f. Feng, H. Pan, *U.S. Patent 8,314,767[P]*, **2012**.
- [58] K. Hong, K. Kim, S. Kim, I. Lee, H. Cho, S. Yoo, H. W. Choi, N.-Y. Lee, Y.-H. Tak, J.-L. Lee, *J. Phys. Chem. C* **2011**, 115, 3453.
- [59] L. Smith, J. Wasey, W. L. Barnes, *Appl. Phys. Lett.* **2004**, 84, 2986.
- [60] Z. Wang, Z. Chen, L. Xiao, Q. Gong, *Org. Electron.* **2009**, 10, 341.
- [61] a) Y.-K. Ee, P. Kumnorkaew, R. A. Arif, H. Tong, J. F. Gilchrist, N. Tansu, *Opt. Express* **2009**, 17, 13747; b) H. Jiang, J. Lin, *J. Korean Phys. Soc.* **2003**, 42, S757; c) W. Knoll, *Curr. Opin. Colloid Interface Sci.* **1996**, 1, 137.
- [62] a) S. Wedge, A. Giannattasio, W. Barnes, *Org. Electron.* **2007**, 8, 136; b) J. M. Lupton, B. J. Matternson, I. D. Samuel, M. J. Jory, W. L. Barnes, *Appl. Phys. Lett.* **2000**, 77, 3340; c) P. Hobson, J. Wasey, I. Sage, W. Barnes, *IEEE J. Sel. Top. Quantum Electron.* **2002**, 8, 378.
- [63] J. M. Ziebarth, A. K. Saafir, S. Fan, M. D. McGehee, *Adv. Funct. Mater.* **2004**, 14, 451.
- [64] L. Li, Z. Yu, C.-h. Chang, W. Hu, X. Niu, Q. Chen, Q. Pei, *Phys. Chem. Chem. Phys.* **2012**, 14, 14249.
- [65] L. Kinner, S. Nau, K. Popovic, S. Sax, I. Burgués-Ceballos, F. Hermerschmidt, A. Lange, C. Boeffel, S. A. Choulis, E. J. List-Kratochvil, *Appl. Phys. Lett.* **2017**, 110, 101107.
- [66] T.-W. Lee, O. O. Park, Y. C. Kim, *Org. Electron.* **2007**, 8, 317.
- [67] N. Corcoran, P. Ho, A. Arias, J. Mackenzie, R. Friend, G. Fichtel, W. Huck, *Appl. Phys. Lett.* **2004**, 85, 2965.
- [68] a) C.-M. Lai, Y.-H. Yeh, Y.-H. Huang, *U.S. Patent Application 11/308, 015[P]*, **2007**; b) T. Sekitani, H. Nakajima, H. Maeda, T. Fukushima, T. Aida, K. Hata, T. Someya, *Nat. Mater.* **2009**, 8, 494; c) A. Tsuboyama, H. Iwawaki, M. Furugori, T. Mukaide, J. Kamatani, S. Igawa, T. Moriyama, S. Miura, T. Takiguchi, S. Okada, *J. Am. Chem. Soc.* **2003**, 125, 12971; d) S. Y. Kim, W. I. Jeong, C. Mayr, Y. S. Park, K. H. Kim, J. H. Lee, C. K. Moon, W. Brütting, J. J. Kim, *Adv. Funct. Mater.* **2013**, 23, 3896; e) T. A. Lin, T. Chatterjee, W. L. Tsai, W. K. Lee, M. J. Wu, M. Jiao, K. C. Pan, C. L. Yi, C. L. Chung, K. T. Wong, *Adv. Mater.* **2016**, 28, 6976;
- f) C. W. Tang, S. A. VanSlyke, C. H. Chen, *J. Appl. Phys.* **1989**, 65, 3610; g) Y. Jiang, D.-Y. Zhou, S.-C. Dong, C. W. Tang, *SID Symp. Dig. Tech. Pap.* **2019**, 50, 252; h) H. Tang, Y. Jiang, C. W. Tang, H.-S. Kwok, *J. Disp. Technol.* **2016**, 12, 605.
- [69] a) S. Reineke, M. Thomschke, B. Lüssem, K. Leo, *Rev. Mod. Phys.* **2013**, 85, 1245; b) N. Patel, S. Cina, J. Burroughes, *IEEE J. Sel. Top. Quantum Electron.* **2002**, 8, 346; c) S. Carter, M. Angelopoulos, S. Karg, P. Brock, J. Scott, *Appl. Phys. Lett.* **1997**, 70, 2067; d) M. Granström, O. Inganäs, *Appl. Phys. Lett.* **1996**, 68, 147; e) Y. Yang, A. Heeger, *Appl. Phys. Lett.* **1994**, 64, 1245; f) Q. Pei, G. Yu, C. Zhang, Y. Yang, A. J. Heeger, *Science* **1995**, 269, 1086; g) Y. Shi, J. Liu, Y. Yang, *J. Appl. Phys.* **2000**, 87, 4254; h) I. D. Parker, *J. Appl. Phys.* **1994**, 75, 1656; i) J. Liang, L. Li, X. Niu, Z. Yu, Q. Pei, *Nat. Photonics* **2013**, 7, 817; j) P. K. H. Ho, J.-S. Kim, J. H. Burroughes, H. Becker, S. F. Y. Li, T. M. Brown, F. Cacialli, R. H. Friend, *Nature* **2000**, 404, 481; k) X. Gong, S. Wang, D. Moses, G. C. Bazan, A. J. Heeger, *Adv. Mater.* **2005**, 17, 2053.
- [70] a) P. Kumar, A. Khanna, S.-Y. Son, J. S. Lee, R. K. Singh, *Opt. Commun.* **2011**, 284, 4279; b) D.-H. Kim, C.-O. Cho, Y.-G. Roh, H. Jeon, Y. S. Park, J. Cho, J. S. Im, C. Sone, Y. Park, W. J. Choi, Q.-H. Park, *Appl. Phys. Lett.* **2005**, 87, 203508; c) T. Fujii, Y. Gao, R. Sharma, E. L. Hu, S. P. DenBaars, S. Nakamura, *Appl. Phys. Lett.* **2004**, 84, 855.
- [71] J. Zhong, H. Chen, G. Saraf, Y. Lu, C. K. Choi, J. J. Song, D. M. Mackie, H. Shen, *Appl. Phys. Lett.* **2007**, 90, 203515.
- [72] Q. Li, K. R. Westlake, M. H. Crawford, S. R. Lee, D. D. Koleske, J. J. Figiel, K. C. Cross, S. Fatholouloumi, Z. Mi, G. T. Wang, *Opt. Express* **2011**, 19, 25528.
- [73] a) H. Dae-Seob, K. Ja-Yeon, N. Seok-In, K. Sang-Hoon, L. Ki-Dong, K. Bongjin, P. Seong-Ju, *IEEE Photonics Technol. Lett.* **2006**, 18, 1406; b) O. B. Shchekin, J. E. Epler, T. A. Trottier, T. Margalith, D. A. Steigerwald, M. O. Holcomb, P. S. Martin, M. R. Krames, *Appl. Phys. Lett.* **2006**, 89, 071109.
- [74] V. Dolores-Calzadilla, B. Romeira, F. Pagliano, S. Birindelli, A. Higuera-Rodriguez, P. J. van Veldhoven, M. K. Smit, A. Fiore, D. Heiss, *Nat. Commun.* **2017**, 8, 14323.
- [75] D. Delbeke, R. Bockstaele, P. Bienstman, R. Baets, H. Benisty, *IEEE J. Sel. Top. Quantum Electron.* **2002**, 8, 189.
- [76] M. R. Krames, H. Amano, J. J. Brown, P. L. Heremans, *IEEE J. Sel. Top. Quantum Electron.* **2002**, 8, 185.
- [77] a) R. K. Ahrenkiel, D. J. Dunlavy, B. Keyes, S. M. Vernon, T. M. Dixon, S. P. Tobin, K. L. Miller, R. E. Hayes, *Appl. Phys. Lett.* **1989**, 55, 1088; b) M. Saliba, W. Zhang, V. M. Burlakov, S. D. Stranks, Y. Sun, J. M. Ball, M. B. Johnston, A. Goriely, U. Wiesner, H. J. Snaith, *Adv. Funct. Mater.* **2015**, 25, 5038; c) H. Benisty, H. D. Neve, C. Weisbuch, *IEEE J. Quantum Electron.* **1998**, 34, 1632; d) T. Kuriyama, T. Kamiya, H. Yanai, *Jpn. J. Appl. Phys.* **1997**, 16, 465; e) Y. Fang, H. Wei, Q. Dong, J. Huang, *Nat. Commun.* **2017**, 8, 14417.
- [78] a) R. Windisch, C. Rooman, S. Meinschmidt, P. Kiesel, D. Zipperer, G. H. Döhler, B. Dutta, M. Kuijk, G. Borghs, P. Heremans, *Appl. Phys. Lett.* **2001**, 79, 2315; b) R. Windisch, B. Dutta, M. Kuijk, A. Knobloch, S. Meinschmidt, S. Schorberth, P. Kiesel, G. Borghs, G. H. Döhler, P. Heremans, *IEEE Trans. Electron Devices* **2000**, 47, 1492; c) P. Shyi-Ming, T. Ru-Chin, F. Yu-Mei, R. Yeh, H. Jung-Tsung, *IEEE Photonics Technol. Lett.* **2003**, 15, 649.
- [79] a) H. Deckman, J. Dunsmuir, *Appl. Phys. Lett.* **1982**, 41, 377; b) C. Haginoya, M. Ishibashi, K. Koike, *Appl. Phys. Lett.* **1997**, 71, 2934; c) H. W. Deckman, J. H. Dunsmuir, *J. Vac. Sci. Technol. B: Microelectron. Nanometer Struct.—Process, Meas., Phenom.* **1983**, 1, 1109; d) R. H. Horng, C. C. Yang, J. Y. Wu, S. H. Huang, C. E. Lee, D. S. Wu, *Appl. Phys. Lett.* **2005**, 86, 221101.
- [80] a) S. G. Johnson, S. Fan, P. R. Villeneuve, J. D. Joannopoulos, L. A. Kolodziejski, *Phys. Rev. B* **1999**, 60, 5751; b) I. V. Shadrivov, A. A. Sukhorukov, Y. S. Kivshar, *Phys. Rev. E*

- 2003, 67, 057602; c) S. Fan, J. N. Winn, A. Devenyi, J. C. Chen, R. D. Meade, J. D. Joannopoulos, *J. Opt. Soc. Am. B* **1995**, 12, 1267; d) F. J. Rodríguez-Fortuño, G. Marino, P. Ginzburg, D. O'Connor, A. Martínez, G. A. Wurtz, A. V. Zayats, *Science* **2013**, 340, 328; e) A. V. Maslov, C. Z. Ning, *Appl. Phys. Lett.* **2003**, 83, 1237; f) S. S. Menon, J. K. Bhalani, S. K. Pathak, presented at 2012 *Int. Conf. on Communication Systems and Network Technologies*, May 2012; g) A. David, T. Fujii, R. Sharma, K. McGroddy, S. Nakamura, S. P. DenBaars, E. L. Hu, C. Weisbuch, H. Benisty, *Appl. Phys. Lett.* **2006**, 88, 061124; h) B.-I. Wu, T. M. Grzegorzczak, Y. Zhang, J. A. Kong, *J. Appl. Phys.* **2003**, 93, 9386.
- [81] a) J. Hu, C. R. Menyuk, *Adv. Opt. Photonics* **2009**, 1, 58; b) R. Zia, M. D. Selker, M. L. Brongersma, *Phys. Rev. B* **2005**, 71, 165431; c) Y. Ding, R. Magnusson, *Opt. Express* **2004**, 12, 1885; d) N. A. Issa, L. Poladian, *J. Lightwave Technol.* **2003**, 21, 1005; e) N. Marcuvitz, *IRE Trans. Antennas Propag.* **1956**, 4, 192; f) E. Anemogiannis, E. N. Glytsis, T. K. Gaylord, *J. Lightwave Technol.* **1999**, 17, 929.
- [82] C. Wiesmann, K. Bergenek, N. Linder, U. T. Schwarz, *Laser Photonics Rev.* **2009**, 3, 262.
- [83] K.-K. Kim, S.-d. Lee, H. Kim, J.-C. Park, S.-N. Lee, Y. Park, S.-J. Park, S.-W. Kim, *Appl. Phys. Lett.* **2009**, 94, 071118.
- [84] a) N.-M. Park, T.-S. Kim, S.-J. Park, *Appl. Phys. Lett.* **2001**, 78, 2575; b) H. An, B. Chen, J. Hou, J. Shen, S. Liu, *J. Phys. D: Appl. Phys.* **1998**, 31, 1144; c) P. M. Fauchet, *Mater. Today* **2005**, 8, 26; d) F. K. Yam, Z. Hassan, *Microelectron. J.* **2005**, 36, 129.
- [85] a) J. Caruge, J. E. Halpert, V. Wood, V. Bulović, M. Bawendi, *Nat. Photonics* **2008**, 2, 247; b) H. M. Haverinen, R. A. Myllylä, G. E. Jabbour, *J. Disp. Technol.* **2010**, 6, 87; c) L. Sun, J. Choi, D. Stachnik, A. C. Bartnik, B.-R. Hyun, G. G. Malliaras, T. Hanrath, F. W. Wise, *Nat. Nanotechnol.* **2012**, 7, 369; d) B. S. Mashford, M. Stevenson, Z. Popovic, C. Hamilton, Z. Zhou, C. Breen, J. Steckel, V. Bulovic, M. Bawendi, S. Coe-Sullivan, *Nat. Photonics* **2013**, 7, 407; e) Y. Shirasaki, G. J. Supran, M. G. Bawendi, V. Bulović, *Nat. Photonics* **2013**, 7, 13; f) S. Nakamura, K. Kitamura, H. Umeya, A. Jia, M. Kobayashi, A. Yoshikawa, M. Shimotomai, Y. Kato, K. Takahashi, *Electron. Lett.* **1998**, 34, 2435; g) S. Coe-Sullivan, *Nat. Photonics* **2009**, 3, 315; h) Y. Jiang, L. Jiang, F. S. Yan Yeung, P. Xu, S. Chen, H.-S. Kwok, G. Li, *ACS Appl. Mater. Interfaces* **2019**, 11, 11119; i) Y. Jiang, S. Chen, H.-S. Kwok, *SID Symp. Dig. Tech. Pap.* **2017**, 48, 161.
- [86] S. Wang, X. Dou, L. Chen, Y. Fang, A. Wang, H. Shen, Z. Du, *Nanoscale* **2018**, 10, 11651.
- [87] X. Yang, K. Dev, J. Wang, E. Mutlugun, C. Dang, Y. Zhao, S. Liu, Y. Tang, S. T. Tan, X. W. Sun, *Adv. Funct. Mater.* **2014**, 24, 5977.
- [88] X. Yang, E. Mutlugun, C. Dang, K. Dev, Y. Gao, S. T. Tan, X. W. Sun, H. V. Demir, *ACS Nano* **2014**, 8, 8224.
- [89] R. Zhu, Z. Luo, S.-T. Wu, *Opt. Express* **2014**, 22, A1783.
- [90] P. Yeh, *Optical Waves in Layered Media*, Wiley Online Library, XXXX 1988.
- [91] H. Liang, R. Zhu, Y. Dong, S.-T. Wu, J. Li, J. Wang, J. Zhou, *Opt. Express* **2015**, 23, 12910.
- [92] a) B. Schwartz, M. Oehme, K. Kostecky, D. Widmann, M. Gollhofer, R. Koerner, S. Bechler, I. A. Fischer, T. Wendav, E. Kasper, J. Schulze, M. Kittler, *Opt. Lett.* **2015**, 40, 3209; b) S. Nakamura, M. Senoh, N. Iwasa, S.-I. Nagahama, *Jpn. J. Appl. Phys.* **1995**, 34, L797.
- [93] a) V. F. Mymrin, K. A. Bulashevich, N. I. Podolskaya, I. A. Zhmakin, S. Y. Karpov, Y. N. Makarov, *Phys. Status Solidi C* **2005**, 2, 2928; b) C. H. Chen, S. J. Chang, Y. K. Su, G. C. Chi, J. K. Sheu, J. F. Chen, *IEEE J. Sel. Top. Quantum Electron.* **2002**, 8, 284.
- [94] S. Nakamura, G. Fasol, *The Blue Laser Diode: Gan Based Light Emitters and Lasers*, Springer Science & Business Media, Berlin **2013**.
- [95] A. Bakin, A. Behrends, A. Waag, H.-J. Lugauer, A. Laubsch, K. Streubel, *Proc. IEEE* **2010**, 98, 1281.
- [96] A. Dadgar, C. Hums, A. Diez, F. Schulze, J. Bläsing, A. Krost, *Proc. SPIE* **2006**, 6355, 63550R.
- [97] S.-M. Kim, T.-Y. Park, S.-J. Park, S.-J. Lee, J. H. Baek, Y. C. Park, G. Y. Jung, *Opt. Express* **2009**, 17, 14791.
- [98] C. Shen, S.-J. Chang, T. Ko, C. Kuo, S.-C. Shei, W. Chen, C.-T. Lee, C. Chang, Y.-Z. Chiou, *IEEE Photonics Technol. Lett.* **2006**, 18, 2517.
- [99] J. W. Lee, D. Y. Kim, J. H. Park, E. F. Schubert, J. Kim, J. Lee, Y.-I. Kim, Y. Park, J. K. Kim, *Sci. Rep.* **2016**, 6, 22537.
- [100] a) S. A. Veldhuis, P. P. Boix, N. Yantara, M. Li, T. C. Sum, N. Mathews, S. G. Mhaisalkar, *Adv. Mater.* **2016**, 28, 6804; b) N. Yantara, S. Bhaumik, F. Yan, D. Sabba, H. A. Dewi, N. Mathews, P. P. Boix, H. V. Demir, S. Mhaisalkar, *J. Phys. Chem. Lett.* **2015**, 6, 4360; c) M.-G. La-Placa, G. Longo, A. Babaei, L. Martínez-Sarti, M. Sessolo, H. J. Bolink, *Chem. Commun.* **2017**, 53, 8707; d) J. W. Choi, H. C. Woo, X. Huang, W.-G. Jung, B.-J. Kim, S.-W. Jeon, S.-Y. Yim, J.-S. Lee, C.-L. Lee, *Nanoscale* **2018**, 10, 13356; e) L. Zhang, X. Yang, Q. Jiang, P. Wang, Z. Yin, X. Zhang, H. Tan, Y. M. Yang, M. Wei, B. R. Sutherland, *Nat. Commun.* **2017**, 8, 15640.
- [101] N. Wang, L. Cheng, R. Ge, S. Zhang, Y. Miao, W. Zou, C. Yi, Y. Sun, Y. Cao, R. Yang, Y. Wei, Q. Guo, Y. Ke, M. Yu, Y. Jin, Y. Liu, Q. Ding, D. Di, L. Yang, G. Xing, H. Tian, C. Jin, F. Gao, R. H. Friend, J. Wang, W. Huang, *Nat. Photonics* **2016**, 10, 699.
- [102] a) Q. Zhou, Z. Bai, W. g. Lu, Y. Wang, B. Zou, H. Zhong, *Adv. Mater.* **2016**, 28, 9163; b) G. Li, F. W. R. Rivarola, N. J. Davis, S. Bai, T. C. Jellicoe, F. de la Peña, S. Hou, C. Ducati, F. Gao, R. H. Friend, *Adv. Mater.* **2016**, 28, 3528; c) X. Zhang, H. Lin, H. Huang, C. Reckmeier, Y. Zhang, W. C. Choy, A. L. Rogach, *Nano Lett.* **2016**, 16, 1415; d) W. G. Lu, X. G. Wu, S. Huang, L. Wang, Q. Zhou, B. Zou, H. Zhong, Y. Wang, *Adv. Opt. Mater.* **2017**, 5, 1700594; e) H. C. Wang, S. Y. Lin, A. C. Tang, B. P. Singh, H. C. Tong, C. Y. Chen, Y. C. Lee, T. L. Tsai, R. S. Liu, *Angew. Chem., Int. Ed.* **2016**, 55, 7924; f) M. Liu, G. Zhong, Y. Yin, J. Miao, K. Li, C. Wang, X. Xu, C. Shen, H. Meng, *Adv. Sci.* **2017**, 4, 1700335.
- [103] L. Polavarapu, B. Nickel, J. Feldmann, A. S. Urban, *Adv. Energy Mater.* **2017**, 7, 1700267.
- [104] a) M. S. Gudixsen, L. J. Lauhon, J. Wang, D. C. Smith, C. M. Lieber, *Nature* **2002**, 415, 617; b) S. Zhao, H. P. T. Nguyen, M. G. Kibria, Z. Mi, *Prog. Quantum Electron.* **2015**, 44, 14; c) R. Könenkamp, R. C. Word, C. Schlegel, *Appl. Phys. Lett.* **2004**, 85, 6004; d) J. K. Hyun, S. Zhang, L. J. Lauhon, *Annu. Rev. Mater. Res.* **2013**, 43, 451.
- [105] a) C. M. Lieber, Z. L. Wang, *MRS Bull.* **2007**, 32, 99; b) Y. Li, F. Qian, J. Xiang, C. M. Lieber, *Mater. Today* **2006**, 9, 18; c) X. Jiang, B. Tian, J. Xiang, F. Qian, G. Zheng, H. Wang, L. Mai, C. M. Lieber, *Proc. Natl. Acad. Sci. USA* **2011**, 108, 12212.
- [106] R. Yan, D. Gargas, P. Yang, *Nat. Photonics* **2009**, 3, 569.
- [107] a) X. Duan, Y. Huang, Y. Cui, J. Wang, C. M. Lieber, *Nature* **2001**, 409, 66; b) Y. Huang, X. Duan, C. M. Lieber, *Small* **2005**, 1, 142; c) Z. Zhong, F. Qian, D. Wang, C. M. Lieber, *Nano Lett.* **2003**, 3, 343; d) E. D. Minot, F. Kelkensberg, M. van Kouwen, J. A. van Dam, L. P. Kouwenhoven, V. Zwiller, M. T. Borgström, O. Wunnicke, M. A. Verheijen, E. P. A. M. Bakkers, *Nano Lett.* **2007**, 7, 367; e) F. Qian, Y. Li, S. Gradečak, D. Wang, C. J. Barrelet, C. M. Lieber, *Nano Lett.* **2004**, 4, 1975.
- [108] a) S. De Franceschi, J. van Dam, E. Bakkers, L. Feiner, L. Gurevich, L. P. Kouwenhoven, *Appl. Phys. Lett.* **2003**, 83, 344; b) M. T. Borgström, V. Zwiller, E. Müller, A. Imamoglu, *Nano Lett.* **2005**, 5, 1439.
- [109] S. Hersee, M. Fairchild, A. Rishinaramangalam, M. Ferdous, L. Zhang, P. Varangis, B. Swartzentruber, A. Talin, *Electron. Lett.* **2009**, 45, 75.
- [110] C. Pan, L. Dong, G. Zhu, S. Niu, R. Yu, Q. Yang, Y. Liu, Z. L. Wang, *Nat. Photonics* **2013**, 7, 752.
- [111] Y.-H. Ra, R. Wang, S. Y. Woo, M. Djavaid, S. M. Sadaf, J. Lee, G. A. Botton, Z. Mi, *Nano Lett.* **2016**, 16, 4608.
- [112] H. P. T. Nguyen, M. Djavaid, K. Cui, Z. Mi, *Nanotechnology* **2012**, 23, 194012.

- [113] D. van Dam, D. R. Abujetas, R. Paniagua-Domínguez, J. A. Sánchez-Gil, E. P. A. M. Bakkers, J. E. M. Haverkort, J. Gómez Rivas, *Nano Lett.* **2015**, *15*, 4557.
- [114] a) T. M. Babinec, B. J. M. Hausmann, M. Khan, Y. Zhang, J. R. Maze, P. R. Hemmer, M. Lončar, *Nat. Nanotechnol.* **2010**, *5*, 195; b) J. Claudon, J. Bleuse, N. S. Malik, M. Bazin, P. Jaffrennou, N. Gregersen, C. Sauvan, P. Lalanne, J.-M. Gérard, *Nat. Photonics* **2010**, *4*, 174; c) M. E. Reimer, G. Bulgarini, N. Akopian, M. Hocevar, M. B. Bavinck, M. A. Verheijen, E. P. A. M. Bakkers, L. P. Kouwenhoven, V. Zwiller, *Nat. Commun.* **2012**, *3*, 737; d) A. Tribu, G. Sallen, T. Aichele, R. André, J.-P. Poizat, C. Bougerol, S. Tatarenko, K. Kheng, *Nano Lett.* **2008**, *8*, 4326; e) S. Deshpande, J. Heo, A. Das, P. Bhattacharya, *Nat. Commun.* **2013**, *4*, 1675; f) I. Friedler, C. Sauvan, J. P. Hugonin, P. Lalanne, J. Claudon, J. M. Gérard, *Opt. Express* **2009**, *17*, 2095; g) M. A. M. Versteegh, M. E. Reimer, K. D. Jöns, D. Dalacu, P. J. Poole, A. Gulinatti, A. Giudice, V. Zwiller, *Nat. Commun.* **2014**, *5*, 5298.
- [115] H.-M. Kim, Y.-H. Cho, H. Lee, S. I. Kim, S. R. Ryu, D. Y. Kim, T. W. Kang, K. S. Chung, *Nano Lett.* **2004**, *4*, 1059.
- [116] a) S. Z. Oener, P. Khoram, S. Brittman, S. A. Mann, Q. Zhang, Z. Fan, S. W. Boettcher, E. C. Garnett, *Nano Lett.* **2017**, *17*, 6557; b) P. Khoram, S. Z. Oener, Q. Zhang, Z. Fan, E. C. Garnett, *Mol. Syst. Des. Eng.* **2018**, *3*, 723.
- [117] H. Zhu, Y. Fu, F. Meng, X. Wu, Z. Gong, Q. Ding, M. V. Gustafsson, M. T. Trinh, S. Jin, X. Zhu, *Nat. Mater.* **2015**, *14*, 636.
- [118] J. Zhao, Y. Yan, C. Wei, W. Zhang, Z. Gao, Y. S. Zhao, *Nano Lett.* **2018**, *18*, 1241.
- [119] Q. Zhang, D. Zhang, L. Gu, K.-H. Tsui, S. Poddar, Y. Fu, L. Shu, Z. Fan, *ACS Nano* **2020**, *14*, 1577.
- [120] a) J.-J. Huang, H.-C. Kuo, S.-C. Shen, *Nitride Semiconductor Light-emitting Diodes (LEDs): Materials, Technologies, and Applications*, Woodhead Publishing, Cambridge, UK **2017**; b) G. Basin, P. S. Martin, *US Patent App. 12/537,909*, **2011**.
- [121] a) C. J. Albergo, R. J. Maryjanowski, M. L. Ott, *US Patent 5,077,587*, **1991**; b) J. K. Kim, S. Chhajed, M. F. Schubert, E. F. Schubert, A. J. Fischer, M. H. Crawford, J. Cho, H. Kim, C. Sone, *Adv. Mater.* **2008**, *20*, 801.
- [122] S. C. Allen, A. Steckl, *J. Disp. Technol.* **2007**, *3*, 155.
- [123] H.-Y. Lin, K.-J. Chen, S.-W. Wang, C.-C. Lin, K.-Y. Wang, J.-R. Li, P.-T. Lee, M.-H. Shih, X. Li, H.-M. Chen, H.-C. Kuo, *Opt. Express* **2015**, *23*, A27.
- [124] J. K. Kim, T. Gessmann, H. Luo, E. F. Schubert, *Appl. Phys. Lett.* **2004**, *84*, 4508.
- [125] M. R. Krames, M. Ochiai-Holcomb, G. E. Höfler, C. Carter-Coman, E. I. Chen, I.-H. Tan, P. Grillot, N. F. Gardner, H. C. Chui, J.-W. Huang, S. A. Stockman, F. A. Kish, M. G. Craford, T. S. Tan, C. P. Kocot, M. Hueschen, J. Posselt, B. Loh, G. Sasser, D. Collins, *Appl. Phys. Lett.* **1999**, *75*, 2365.
- [126] V. Zabelin, D. A. Zakheim, S. A. Gurevich, *IEEE J. Quantum Electron.* **2004**, *40*, 1675.
- [127] J. J. Wierer, D. A. Steigerwald, M. R. Krames, J. J. O'Shea, M. J. Ludowise, G. Christenson, Y.-C. Shen, C. Lowery, P. S. Martin, S. Subramanya, W. Götz, N. F. Gardner, R. S. Kern, S. A. Stockman, *Appl. Phys. Lett.* **2001**, *78*, 3379.
- [128] C. E. Lee, Y. C. Lee, H. C. Kuo, M. R. Tsai, T. C. Lu, S. C. Wang, *Semicond. Sci. Technol.* **2008**, *23*, 025015.
- [129] R. Ji, M. Hornung, M. A. Verschuuren, R. van de Laar, J. van Eekelen, U. Plachetka, M. Moeller, C. Moormann, *Microelectron. Eng.* **2010**, *87*, 963.
- [130] M. R. Tan, D. A. Fattal, M. Fiorentino, S.-Y. Wang, *US Patent 9,263,637*, **2016**.
- [131] C. Lee, Y. Lee, H. Kuo, M. Tsai, B. S. Cheng, T. Lu, S. Wang, C. Kuo, *IEEE Photonics Technol. Lett.* **2007**, *19*, 1200.
- [132] C. H. Liu, R. W. Chuang, S. J. Chang, Y. K. Su, L. W. Wu, C. C. Lin, *Mater. Sci. Eng., B* **2004**, *112*, 10.
- [133] a) H. Telfah, A. Jamhawi, M. B. Teunis, R. Sardar, J. Liu, *J. Phys. Chem. C* **2017**, *121*, 28556; b) M. Lorenzon, L. Sortino, Q. Akkerman, S. Accornero, J. Pedrini, M. Prato, V. Pinchetti, F. Meinardi, L. Manna, S. Brovelli, *Nano Lett.* **2017**, *17*, 3844; c) Y. Fu, H. Zhu, J. Chen, M. P. Hautzinger, X. Y. Zhu, S. Jin, *Nat. Rev. Mater.* **2019**, *4*, 169.
- [134] a) J. Li, P. Du, S. Li, J. Liu, M. Zhu, Z. Tan, M. Hu, J. Luo, D. Guo, L. Ma, Z. Nie, Y. Ma, L. Gao, G. Niu, J. Tang, *Adv. Funct. Mater.* **2019**, *29*, 1903607; b) Y. Hu, Q. Wang, Y.-L. Shi, M. Li, L. Zhang, Z.-K. Wang, L.-S. Liao, *J. Mater. Chem. C* **2017**, *5*, 8144; c) A. Genco, F. Mariano, S. Carallo, V. L. P. Guerra, S. Gambino, D. Simeone, A. Listorti, S. Colella, G. Gigli, M. Mazzeo, *Adv. Electron. Mater.* **2016**, *2*, 1500325; d) F. Mariano, A. Listorti, A. Rizzo, S. Colella, G. Gigli, M. Mazzeo, *Appl. Phys. Lett.* **2017**, *111*, 163301.
- [135] M. Koden, *OLED Displays and Lighting*, John Wiley and Sons, Chichester, UK **2017**, p. 103.
- [136] J.-H. Im, C.-R. Lee, J.-W. Lee, S.-W. Park, N.-G. Park, *Nanoscale* **2011**, *3*, 4088.
- [137] Y. Wang, X. Li, J. Song, L. Xiao, H. Zeng, H. Sun, *Adv. Mater.* **2015**, *27*, 7101.
- [138] M. Leng, Z. Chen, Y. Yang, Z. Li, K. Zeng, K. Li, G. Niu, Y. He, Q. Zhou, J. Tang, *Angew. Chem., Int. Ed.* **2016**, *55*, 15012.
- [139] F. Liu, Y. Zhang, C. Ding, S. Kobayashi, T. Izuishi, N. Nakazawa, T. Toyoda, T. Ohta, S. Hayase, T. Minemoto, K. Yoshino, S. Dai, Q. Shen, *ACS Nano* **2017**, *11*, 10373.
- [140] a) H. Spreitzer, H. Becker, E. Kluge, W. Kreuder, H. Schenk, R. Demandt, H. Schoo, *Adv. Mater.* **1998**, *10*, 1340; b) I.-N. Kang, D.-H. Hwang, H.-K. Shim, T. Zyung, J.-J. Kim, *Macromolecules* **1996**, *29*, 165.
- [141] a) S. van Mensfoort, M. Carvelli, M. Megens, D. Wehenkel, M. Bartyzel, H. Greiner, R. Janssen, R. Coehoorn, *Nat. Photonics* **2010**, *4*, 329; b) K. A. Neyts, *J. Opt. Soc. Am. A* **1998**, *15*, 962; c) H. Greiner, O. J. Martin, *Proc. SPIE* **2004**, *5214*, 248.
- [142] S.-j. Lee, A. Badano, J. Kanicki, *IEEE J. Sel. Top. Quantum Electron.* **2004**, *10*, 37.
- [143] C. Qin, T. Matsushima, W. J. Potscavage, A. S. Sandanayaka, M. R. Leyden, F. Bencheikh, K. Goushi, F. Mathevet, B. Heinrich, G. Yumoto, Y. Kanemitsu, C. Adachi, *Nat. Photonics* **2020**, *14*, 70.
- [144] J.-S. Kim, P. K. H. Ho, N. C. Greenham, R. H. Friend, *J. Appl. Phys.* **2000**, *88*, 1073.
- [145] M. Furno, R. Meerheim, S. Hofmann, B. Lüsse, K. Leo, *Phys. Rev. B* **2012**, *85*, 115205.
- [146] Q. Zhao, J. Zhou, F. Zhang, D. Lippens, *Mater. Today* **2009**, *12*, 60.
- [147] A. I. Väkeväinen, R. J. Moerland, H. T. Rekola, A. P. Eskelinen, J. P. Martikainen, D. H. Kim, P. Törmä, *Nano Lett.* **2014**, *14*, 1721.
- [148] X. Li, S. He, Y. Jin, *Phys. Rev. B* **2007**, *75*, 045103.
- [149] H. Jeong, J.-H. Kim, C.-H. Hong, E.-K. Suh, M. S. Jeong, *Opt. Mater. Express* **2015**, *5*, 1306.
- [150] Q. Wang, Q.-S. Tian, Y.-L. Zhang, X. Tang, L.-S. Liao, *J. Mater. Chem. C* **2019**, *7*, 11329.